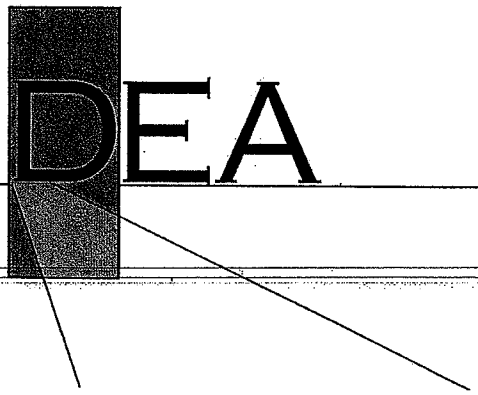

Innovations Deserving
Exploratory Analysis Programs

Highway IDEA Program

Development of an Innovative Connector System for Fiber Reinforced Polymer Bridge Decks to Steel Stringers

Final Report for Highway IDEA Project 66

Prepared by:
Karl E. Barth, Julio F. Davalos, and Jennifer E. Righman,
West Virginia University, Morgantown, WV

August 2003

TRANSPORTATION RESEARCH BOARD
OF THE NATIONAL ACADEMIES

INNOVATIONS DESERVING EXPLORATORY ANALYSIS (IDEA) PROGRAMS
MANAGED BY THE TRANSPORTATION RESEARCH BOARD (TRB)

This NCHRP-IDEA investigation was completed as part of the National Cooperative Highway Research Program (NCHRP). The NCHRP-IDEA program is one of the four IDEA programs managed by the Transportation Research Board (TRB) to foster innovations in highway and intermodal surface transportation systems. The other three IDEA program areas are Transit-IDEA, which focuses on products and results for transit practice, in support of the Transit Cooperative Research Program (TCRP), Safety-IDEA, which focuses on motor carrier safety practice, in support of the Federal Motor Carrier Safety Administration and Federal Railroad Administration, and High Speed Rail-IDEA (HSR), which focuses on products and results for high speed rail practice, in support of the Federal Railroad Administration. The four IDEA program areas are integrated to promote the development and testing of nontraditional and innovative concepts, methods, and technologies for surface transportation systems.

For information on the IDEA Program contact IDEA Program, Transportation Research Board, 500 5th Street, N.W., Washington, D.C. 20001 (phone: 202/334-1461, fax: 202/334-3471, http://www.nationalacademies.org/trb/idea)

The project that is the subject of this contractor-authored report was a part of the Innovations Deserving Exploratory Analysis (IDEA) Programs, which are managed by the Transportation Research Board (TRB) with the approval of the Governing Board of the National Research Council. The members of the oversight committee that monitored the project and reviewed the report were chosen for their special competencies and with regard for appropriate balance. The views expressed in this report are those of the contractor who conducted the investigation documented in this report and do not necessarily reflect those of the Transportation Research Board, the National Research Council, or the sponsors of the IDEA Programs. This document has not been edited by TRB.

The Transportation Research Board of the National Academies, the National Research Council, and the organizations that sponsor the IDEA Programs do not endorse products or manufacturers. Trade or manufacturers' names appear herein solely because they are considered essential to the object of the investigation.

Development of an Innovative Connector System for Fiber-Reinforced Polymer Bridge Decks to Steel Stringers

Executive Summary

FRP bridge decks offer several favorable advantages for bridge construction and particularly rehabilitation projects. Their lightweight, high strength, and non-corrosive characteristics makes them suitable for bridge deck applications. In addition, FRP bridge decks can be manufactured as modular components for rapid installation as new structures and replacement of existing conventional decks, such as concrete.

In the last five years, several research-industry-government teams have demonstrated the feasibility of field applications of FRP decks and bridges for relatively short-spans. Based on cost considerations, it is likely that most FRP structural components will be manufactured from low-cost fibers (E-glass) and resins (Epoxy, Vinyl- ester). Due to the relatively low stiffness of these materials, it appears as though the largest potential market for FRP decks is their installation over steel or concrete stringers for new and retrofit construction of highway bridges. But for this to be possible, *a key problem that requires resolution is the connection of the FRP deck to the supporting stringers; this very important problem is the concern of this project.*

This report focuses on the development and evaluation of a new connector system to attach fiber reinforced polymer (FRP) bridge decks to supporting steel stringers. The proposed connection consists of a threaded shear stud welded to the top flange of the supporting girder and housed inside of steel sleeves that are installed within a hole drilled through the FRP deck. The top steel sleeve is fabricated with a fixed inner washer near

mid-height that provides bearing area to tighten a nut against and a second top washer acts to clamp the deck in place as the nut is tightened.

These prototype connections were first tested using modified direct shear tests. From these tests, ultimate shear strength, load vs. displacement response, mode of failure, and general performance of the connection were determined. In this phase of testing, several variations of the connection were evaluated in order to determine the most suitable connection design.

After selecting a final connection design, the connection was implemented in a reduced scale bridge. The bridge consists of three simply supported W24 x 55 steel beams with a span length of 24 ft, three FRP deck panels approximately 9 ft-9 in. by 8 ft, and 21 of the selected connections with 7 connections per girder spaced at approximately 4 ft intervals. In these tests, load was applied to the center of the bridge and resulting reactions at each support and deflections at key points in the superstructure were recorded. A finite element model of this bridge was also created and the results were correlated with those from the experimental testing. This model will then aid in future efforts related to the use of this connector.

Following the successful development and evaluation of the proposed connector, we will work closely with the WVDOT and KDOT to implement this concept in future bridge projects. In particular, the WVDOT is in the process of implementing a large-scale program for several demonstration bridges in WV using high-performance materials and is very much interested in the immediate implementation of this connector design in order to rapidly advance the effective applications of FRP bridge decks.

TABLE OF CONTENTS

LIST OF TABLES

LIST OF FIGURES

Chapter 1

INTRODUCTION

1.1 Background

Fiber reinforced polymer (FRP) is a promising product for use in bridge construction due to its lightweight and high-strength characteristics, in combination with favorable durability and resistance to corrosion. As a result, the use of FRP in bridge applications has been a source of much investigation in recent years. One of the most likely uses of this material in future bridges is FRP bridge decks over steel or concrete girders. In this situation, FRP sandwich panels or pultruded sections take the place of traditional steel reinforced concrete slabs.

FRP bridge decks can be particularly useful in the growing area of rehabilitation projects. According to one survey, 29% of our nation's bridges are currently in need of repair or replacement (American Society of Civil Engineers, 2001). Often, due to unfavorable condition assessments, a particular bridge may be "posted" for reduced live-load capacity. FRP decks are attractive in these kinds of applications as they may be used in deck replacements to decrease the total dead-load, which is often a significant percentage of the total load demand.

FRP bridge decks offer a number of other advantages. For example, they are resistant to corrosion, they may be placed very rapidly compared to typical cast-in-place

reinforced concrete decks and they offer excellent energy absorption characteristics.

Presently, the major concern with FRP decks in the bridge industry is its initial higher price compared to that of a concrete deck. However, the higher cost of FRP may me justified by considering life-cycle costs; the added durability and corrosion resistance will enhance the deck performance and reduce the need for deck replacements. Also, as FRP becomes more widely used, production quantities and manufacturing advances will help to reduce individual project costs.

Due to the numerous benefits of FRP bridge decks, several states have designed and constructed these types of bridges with favorable results. The majority of the constructed bridges consist of FRP decks supported by steel girders. These bridges are designed as non-composite structures; they rely on the steel girders to support longitudinal shear and bending stresses due to dead and live loads, with the deck acting as a mechanism to support vehicular live load and distribute this to the supporting girders. At present, the idea of composite action in these types of systems is a controversial issue. As the coefficient of thermal expansion is greatly different for steel and FRP and the modular ratio, E_{steel} / E_{FRP}, is quite high, it is assumed in this present effort that the most logical way to continue to design these systems is non-compositely.

One of the present problems with FRP decks is the need to develop an adequate and reliable connection between the deck and the girder. Several proprietary connection methods have been developed and implemented in FRP bridge deck projects with varying degrees of success. However, the strength and long-term performance of these connections has not been thoroughly investigated.

1.2 Description of FRP Decks

Two primary types of FRP decks are currently used in bridge applications; these are pultruded decks and sandwich decks. Pultruded decks consist of pultruded FRP sections that are then bonded together with adhesive to form the bridge deck. There are currently two primary manufacturers of this type of deck: Creative Pultrusions, which manufactures Superdeck^{TM}, and Martin Marietta Composites, which manufactures Duraspan bridge decks (Market Development Alliance, 2000).

Superdeck is composed of two different pultruded shapes, a "truss" section and a "hexagonal" section (see Fig. 1.1). These sections are manufactured using multi-axial stitched fabrics, continuous roving and continuous fiber mats of E-glass fibers and vinyl ester resin. Bonding these two sections together in an alternating pattern then creates the Superdeck.

Duraspan decks consist of two different trapezoidal shaped pultruded sections that are mirror images of one another (see Fig. 1.2). The constituent materials of these sections are E-glass fibers stitched into multi-ply fabrics and isophthalic polyester resin. Similar to Superdeck, the Duraspan deck is then formed by bonding these two sections together in an alternating pattern.

Sandwich panels are the second type of FRP deck commonly used. These decks consist of exterior face sheets (or face skins) separated by a core. The face sheets provide the majority of the bending strength in these types of panels, while the core acts to increase the moment of inertia and to resist shear forces. Currently, there are three manufacturers of this type of bridge deck: Kansas Structural Composites, Inc. (KSCI),

3TEX, Inc., and Hardcore Composites (Market Development Alliance 2000).

Figure 1.3 shows the geometry of the KSCI panels. The top and bottom face sheets are manufactured using hand lay-up and consist of E-glass fibers and polyester resin. The honeycomb core consists of flat and sinusoidal shaped corrugations. These are also manufactured using hand lay-up and the sinusoidal shaped corrugations are created using molds.

The TYCOR bridge deck manufactured by 3TEX, Inc. is shown in Fig. 1.4. The face sheets of these decks are made of a combination of knitted and woven fabrics and the core of the panels contains glass fiber rovings forming a triangulated reinforcing structure. The voids within the core are filled with patented fiber reinforced foam, which is a low-density foam that provides additional reinforcement in the vertical direction.

A schematic diagram of the bridge deck manufactured by Hardcore Composites is shown in Fig. 1.5. These decks are manufactured from E-glass fabrics and vinyl ester resins using a vacuum assisted resin transfer molding. The core of these panels is a low-density cellular type core.

For a more detailed discussion on FRP bridge decks, the reader is directed to a recent review article by Bahis et al. (2002).

1.3 Objectives and Scope of Work

The primary purpose of this study is to develop an improved method for connecting FRP bridge decks to steel girders, as well as to experimentally validate the performance of the new connection design. The goal is to develop an economical,

durable, and reliable means of providing a positive connection from the deck to the steel stringer. The scope of this project includes the conceptual development of a new connection and both experimental and analytical studies of the connection performance.

Specifically, once a new connection is developed, component level testing of individual connections is performed, including testing of several variations of the connection in order to determine the most appropriate design. Then system level tests are conducted that implement the selected connection in a reduced-scale model bridge. This bridge system is loaded statically in order to assess the system performance of the selected connections, as well as to investigate load distribution characteristics. A finite element modeling of the scale model bridge is formulated in order to assist in future efforts related to investigating load distribution characteristics for other girder configurations.

As a result of these efforts, it is expected that the reliable performance of the proposed connection will be experimentally and analytically verified, resulting in the possible implementation of this connection in future projects involving FRP bridge decks. This work is part of a project that is being sponsored by the National Academy of Sciences under the NCHRP-IDEA program.

1.4 Overview of Study

The purpose of this study is to develop and evaluate, both experimentally and analytically, the performance of a new connector for FRP bridge decks to steel bridge girders.

As FRP bridge decks are a relatively new structural system, there is little literature available that discusses testing of connections for this type of bridge deck. However, shear stud connections used in the construction of bridges with steel girders and concrete decks have been studied extensively. Because the behavior of the proposed connection for FRP decks is conceptually similar to these shear stud connections, a critical literature review related to experimental testing of shear stud connections is presented in Chapter 2. The results of this review are then used to formulate a testing method for the new connection. Also presented in Chapter 2 is a discussion of other types of connections that have been used with previously constructed FRP bridge decks.

Chapter 3 discusses the conceptual development of the proposed connection. This chapter introduces the proposed connection as well as the criteria used in its formulation. Once a preliminary conceptual design of the connector has been developed, finite element analysis (FEA) is employed to aid in selecting appropriate dimensions. Details of the FEA and selected dimensions are also given in this chapter.

Static testing of the proposed connection is presented in Chapter 4. In this chapter, four variations of the preliminary connection design are investigated in order to determine the most appropriate design. The scope of this phase of testing includes: determining the ultimate shear strength of individual connections, understanding the mode of failure and type of damage incurred by the connections, assessing the relative performance of the different type of connections investigated, and selecting a final design of the connection to be used in subsequent system level testing.

The experimental testing of the scale model bridge is presented in Chapter 5. Information related to the test setup, instrumentation, and results is provided. The

purpose of this testing is to evaluate the system performance of the connections as well as to investigate the load distribution characteristics that result from use of this connection. This testing consists of statically loading the model bridge with a servo-hydraulic actuator and recording resulting reactions and deflections at key points in the superstructure.

Chapters 6 presents the development of finite element modeling tools that are developed in order to predict resulting reactions and deflections for other superstructure configurations. Several modeling techniques are employed to determine the methods most accurate at capturing the response of the bridge used in the experimental study and a detailed description of the finite element model selected is presented. Results from the finite element model are compared with the experimental results and a discussion of this comparison is also included.

Lastly, Chapter 7 discusses conclusions and recommendations for future work related to this research.

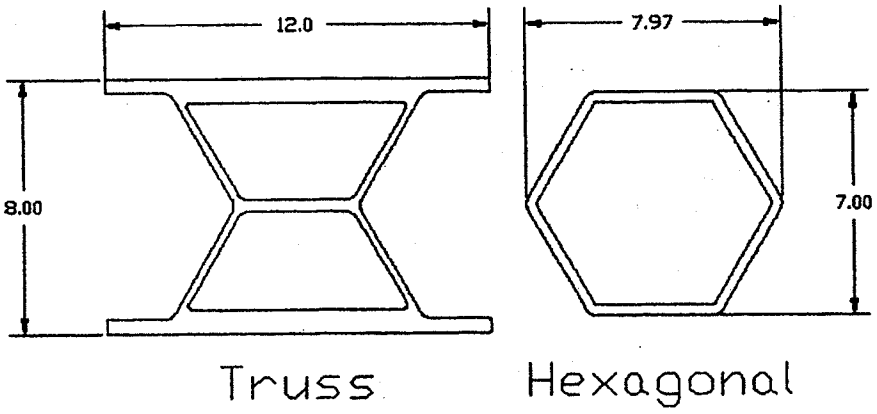

Figure 1.1: Superdeck™ Pultruded Components
(Dimensions in inches)

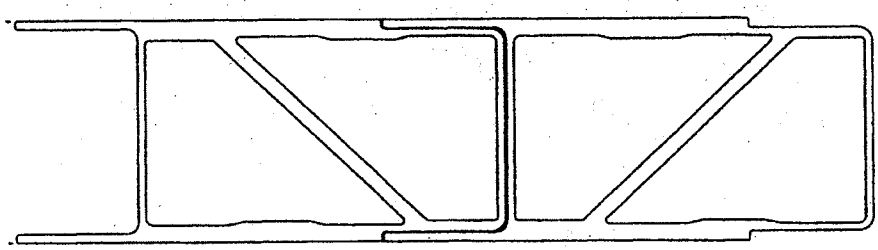

Figure 1.2: Pultruded Components of Duraspan
Bridge Deck

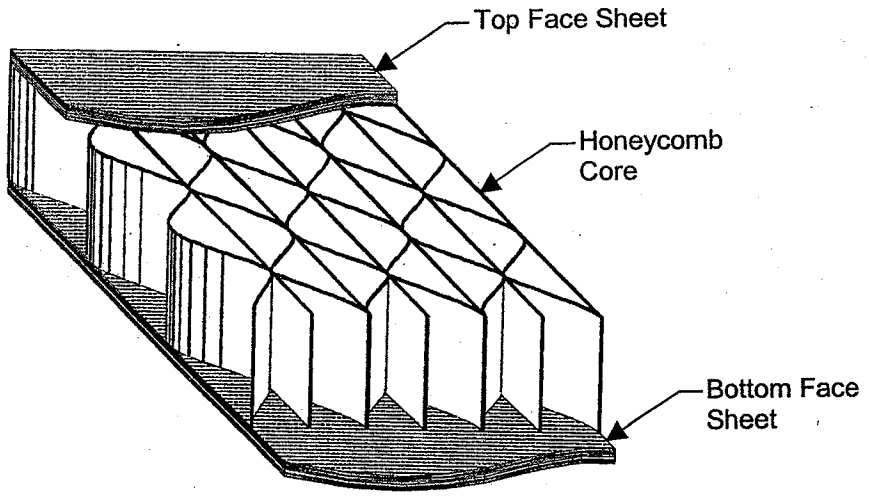

Figure 1.3: Schematic Diagram of FRP Bridge Deck Panel Manufactured By KSCI

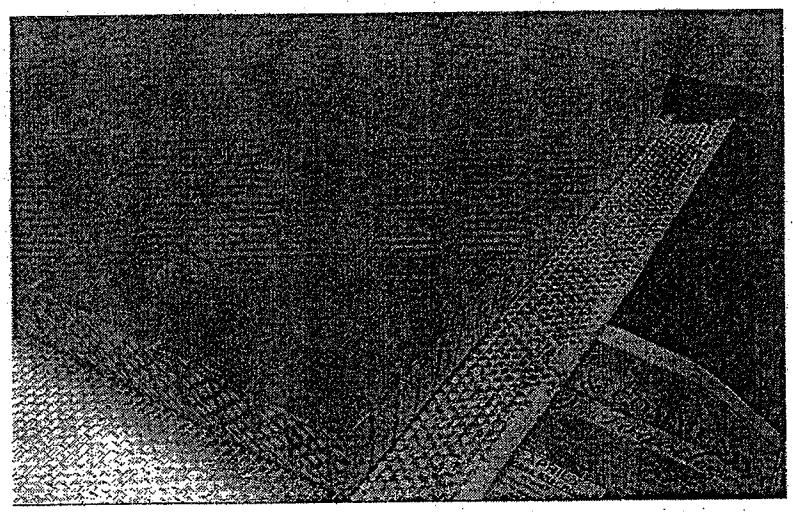

Figure 1.4: Photograph of TYCOR Bridge Deck Panel Manufactured by 3TEX, Inc.

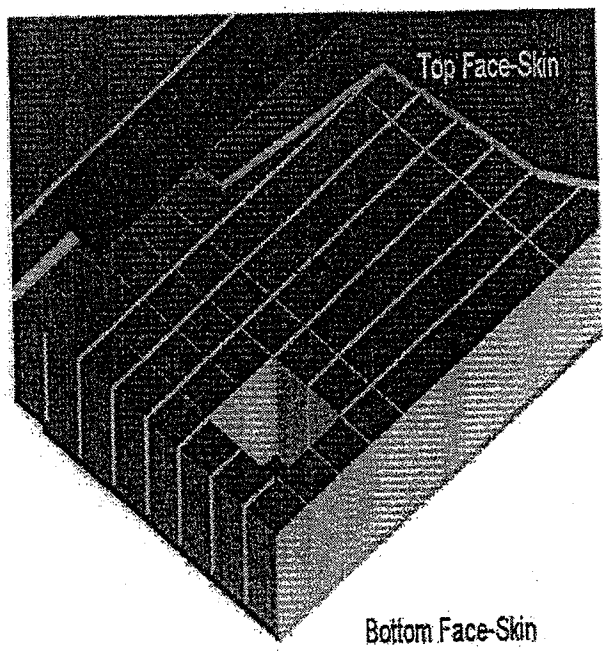

Figure 1.5: Schematic Diagram of Bridge Deck Panel Manufactured by Hardcore Composites

Chapter 2

LITERATURE REVIEW

Abstract

While FRP bridge decks are the source of much recent and ongoing research, little research has been performed regarding the connection between these decks and the supporting girders. Alternatively, a considerable amount of research has been performed to investigate the performance and strength characteristics of shear connectors, used to connect reinforced concrete bridge decks to steel girders. This is of interest because the behavior of these shear connectors is conceptually similar to that of the proposed connection for FRP bridge decks to steel girders that is the focus of this project. Consequently, a summary of this previous research, which has focused on determining factors that influence stud behavior in order to determine mathematical relationships to be used in design, is presented. Testing methods, a description of shear stud behavior, significant results regarding both the static and fatigue strength of shear studs, and conclusions are presented. In addition, a discussion of connections currently used with FRP bridge decks and steel girders is also presented.

2.1 Introduction

Headed shear studs are routinely used in the construction of steel-concrete composite beams in both buildings and bridges. Concrete-steel composite beams consist of a steel rolled beam or plate girder supporting a reinforced-concrete slab that is integrally connected by some type of shear connection, most typically headed shear studs. An additional component sometimes present in composite beams is formed steel deck, which is often used to create a form for the concrete slab.

In order to construct these beams, studs are welded to the top of the steel girder before the concrete slab is poured. When the slab is poured and the concrete hardens, the steel girder and the concrete slab then act as one integrated section. The shear studs act as a mechanism to transfer horizontal shear forces between the concrete bridge deck and the steel girders and additionally to prevent vertical separation between the beam and the slab. This is conceptually similar to the behavior of the connection proposed in this study to attach FRP bridge decks to steel girders.

2.2 Testing Methods

Various testing methods have been adopted in order to investigate the strength characteristics and behavior of shear connectors. Of these, the most popular are beam tests and push-out tests. More recently, researchers have introduced a direct shear test, which is also of interest.

2.2.1 Beam Tests

Beam test specimens are full or reduced-scale composite beams that are representative of an actual girder (Fig. 2.1). These specimens consist of the components of a composite beam including a steel beam, concrete slab, shear connectors and formed steel deck when applicable. Beam tests offer the distinct advantage that any type of loading can be applied or approximated. Additionally, this type of testing is the most accurate method to predict the actual behavior of a composite beam. Beam tests also allow for a wide variety of results to be obtained including ultimate flexural capacity as well as stress and strain at any location desired.

2.2.2 Push-Out Tests

Push-out tests are widely used in experimental testing due to three primary advantages offered over other procedures. These are cost effectiveness, ease in variation of test parameters, and ease in determining the capacity of a single connector.

A typical push-out test configuration is shown in Fig. 2.2. The test specimen consists of two concrete slabs each connected to a flange of the steel I-beam by shear connectors. The concrete slabs are cast so that they extend approximately 2" beyond one end of the beam. This is done so that when the specimen is inverted the slabs rest on the floor, thus supporting the beam. Typically the slabs are secured to the floor by some means (such as grout) to prevent the slabs from splaying. Vertical loads are then applied to the beam while slip between the beam and the slab is measured.

An alternative, yet conceptually similar, type of push-out specimen is shown in Fig. 2.3. The primary difference of this specimen is that only one slab is used. Also, when this type of specimen is selected the load is applied to the slab instead of the beam. Results from these two variations of push-out testing are comparable and used interchangeably (Oehlers and Foley, 1985).

The number of shear connectors used in each slab varies among researchers and testing objectives, with nearly all using one to four connectors per slab. The most common situation is to arrange the shear connectors in one or two transverse rows with two connectors per row. In the analysis of 110 push-out tests, Oehlers and Johnson (1987) found that specimens with a single row of connectors per slab had little ability to redistribute the shear forces between connectors and therefore failed at the strength of the weakest connection. Conversely, specimens with two rows of connectors did redistribute the shear load and hence failed at the average connection strength.

Over the years numerous researchers have investigated the validity of push-out tests. The work of Slutter and Fisher (1966) seemed to verify their accuracy. A comparison between push-out tests and beam tests showed the lower limit of dispersion for the beam tests overlapped the upper limit of dispersion for the push-out tests (Fig. 2.4). Also, the lower limit of dispersion of the beam tests is approximately equal to the average behavior of the push-out specimens thus, it was concluded push-out tests represent a lower bound of connector failure.

Mainstone and Menzies (1967) also examined the accuracy of push-out tests. They believed that it should not be assumed that push-out tests accurately reproduce the actual conditions in the bridge deck without further researching the validity of this testing

technique. Thus, they performed independent testing to confirm push-out test results. In a study focused on shear stud fatigue capacity, push-out tests constituted the bulk of the experimental testing which were confirmed by a refined set of beam tests. Comparisons of the results showed that both slip and ultimately the fatigue failure were generally similar for both types of testing (except for the case of reversed shear). However, the values for connection strength obtained by push-out tests were slightly less than those of the beam tests, agreeing with the previous results of Slutter and Fisher. While this could be interpreted as the push-out tests gave a conservative estimate of strengths that may be obtained, the authors believed that the push-out tests were not sufficiently representative of the conditions in a beam (Mainstone and Menzies, 1967). Consequently, in their recommendations for allowable loads on the shear connectors studied, they placed greater emphasis on the results from the beam studies.

Jayas and Hosain (1988, 1989) shared the opinion that push-out testing should not be solely relied upon and followed a similar testing procedure using push-out tests in preliminary research and then confirming their results by a limited number of beam tests. From a series of push-out tests, the authors established two separate empirical equations to calculate the shear capacity of shear studs for two different metal deck profiles. In subsequent beam tests, they found that there was good agreement between the actual flexural capacity of the beam and that calculated using the stud shear strength previously determined in push-out tests. Figure 2.5 illustrates these results for the study of flexural capacity as related to variable concrete strength and profile of decking.

The views of Easterling et al. (1993) summarize the current opinion on the effectiveness and accuracy of push-out testing. They believe that in order to determine

the strength of individual connectors, push-out testing is the most accurate method. If beam tests alone are used, the sensitivity of stud strength to various parameters is difficult to discern. Additionally, obtaining the load applied to an individual connector can be a complex process of back calculation compared to the simple, direct calculations made when using push-out test specimens. They believe that the best approach is to use a combination of the two methods, using push-out tests initially to evaluate various parameters and form strength relationships and subsequent beam tests as a means to confirm the results.

2.2.3 Direct Shear Test

Gattesco and Giuriani (1996) recently proposed an innovative testing method for use in the study of shear connectors subjected to cyclic loads. They believe an alternative to push-out testing is needed for the case of cyclic loading (especially reverse cyclic loading) due to "limitations and modeling inaccuracies". As a result, they developed the direct shear test.

In a direct shear test load is alternately applied to both sides of the connection, differing from the unidirectional load applied in push-out testing. This allows for fatigue cracks to propagate from both sides of the shear stud, more accurately simulating the actual conditions of shear studs subjected to reverse cyclic loading. A schematic diagram of the test configuration is shown in Fig. 2.6. The test specimens consist of one single shear stud welded to a steel element in order to obtain direct information about individual

connector behavior. Shear forces are transmitted to the steel element and concrete block by means of a dynamic testing machine.

Their study incorporated specimens subjected to monotonically increasing loads for the purpose of comparing results between push-out and direct shear tests. Figure 2.7 illustrates this comparison by showing the empirical equation for shear load ratio vs. slip (labeled as Equation1) derived by Gattesco and Giuriani as the best fit of the test data from two direct shear test specimens, M1 and M2, compared to the push-out test results of two other researchers (Menzies, 1971 and Buttry, 1966). From this data it is clear that the results of the two testing methods are comparable, therefore validating the testing method.

2.3 Composite Action

One of the key parameters influencing shear stud behavior is the level of composite action that is developed. Therefore, this section provides a brief overview of this topic. Composite action refers to the degree that horizontal shear forces are transferred between the beam and the slab. In a section with full composite action, 100% of the horizontal shear forces are transferred between the beam and the slab; conversely, in a non-composite beam there is no transfer of horizontal shear forces. Additionally, a third intermediate situation, termed partial composite action, may exist where some portion of horizontal shear forces are transferred. The amount of composite action that exists in any section is directly related to the amount of shear connection provided.

The degree of composite action that exists significantly affects the behavior of the composite section. When there is no composite action and the section is subjected to some arbitrary vertical loading, the bottom surface of the slab is in tension and elongates while the top surface of the beam is in compression and will shorten. Thus slip occurs between the two surfaces. In the case that some degree of composite action exists the amount of slip will be reduced; in a full composite section there is no slip between the two surfaces (see Fig. 2.8).

2.4 Shear Stud Behavior

Early research on the topic of shear connectors aimed to accurately predict the strength of these connections. As a result of these studies, valuable information regarding the behavior of shear studs under static loading conditions was obtained. One such study was that of Newmark et al. (1951) who studied the behavior of composite beams with partial shear connection. Beam test specimens for this study consisted of simply supported rolled steel I-beams of varying length with concrete slabs connected by channel shear connectors. Loading on the specimens consisted of a single concentrated load applied at various positions along the span. One of the parameters investigated during Newmark's research was variable vs. uniform spacing of the shear connectors.

For the specimens with variable connector spacing, the spacing varied from a maximum near midspan to a minimum at the ends of the beam. These specimens showed that the shear connectors near the ends of the beam resisted more load per unit length than shear connectors near midspan. This is illustrated in Fig. 2.9a by assuming the

amount of slip for a given connector is proportional to the amount of load resisted by that connector. As the amount of slip is similar for locations near the end of the beam and midspan it is assumed that the total load resisted is also similar. Since the connector spacing is less at the end of the beam, thus there is more load per unit length transmitted at the ends of the beam.

In both the specimens with variable and uniform connector spacing, the spacing of the connectors at midspan was consistent at 18". Comparing the results of the uniform and variable spacing tests (Fig. 2.9 a and b), shows that the values of slip at midspan were similar. This suggests that the closer spacing of connectors near the ends of the beam in the variable spacing specimens influenced the end sections only.

Similar tests subsequently conducted by Viest et al. (1952) established that at low static loads the behavior of shear connectors is most like that of a flexible elastic dowel on an elastic foundation. Later studies, including that of Hawkins (1973), confirmed that stress-slip relationships computed using this approach agree closely with experimental results. Figure 2.10 illustrates this by comparing theoretical and measured values of shear stress vs. slip for two tests performed by Hawkins.

Research by Grant et al. (1977) established the ductile behavior of shear connectors. This was demonstrated by the large deflections occurring in the composite beam specimens tested, which were typically ten times the deflection at working load. Such large deflections were permitted by the development of a plastic hinge near midspan. According to Grant et al., the formation of plastic hinges could have only been possible with a ductile shear connection, which permitted redistribution of the slab force along the beam.

2.5 Static Strength of Shear Studs

2.5.1 Strength of Connectors

Numerous studies have been performed in order to determine the parameters that affect the static strength of shear studs and from this information to formulate expressions to easily calculate this strength. One of the most noteworthy of these is that of Ollgaard et al. (1971). This research lead to determination of an expression for the static capacity of shear studs that is accepted by several current codes of practice including the AISC Manual of Steel Construction (Load and Resistance Factor Design) (1998), AASHTO Standard Specifications for Highway Bridges (1996), and AASHTO LRFD Bridge Design Specifications (1998).

Numerous variables were investigated in the study including material characteristics (e.g., concrete properties such as compressive strength, split tensile strength, modulus of elasticity and density as well as stud tensile strength, and type of aggregate used), stud diameter, and number of connectors per slab. Testing was performed using push-out tests, with most specimens having four connectors per slab. Stud sizes used in Ollgaard's testing were based on requirements determined by Slutter and Driscoll (1965) who determined that the height to diameter ratio for studs embedded in normal-weight concrete should be greater than or equal to four in order for the full capacity of the connector to be developed.

After the testing had been completed, several regression analyses were performed to determine a mathematical relationship between the test parameters and the shear

strength of stud connectors. Results showed that the shear strength of the connector was influenced by the cross-sectional area of the connectors (A_s), the compressive strength of the concrete (f'_c), and the modulus of elasticity of the concrete (E_c) and that the other variables investigated (e.g., concrete density and split tensile strength) do not have a significant effect. The following empirical formula best describes the ultimate stud capacity, Qu, based on the test results.

$$Q_u = 1.106 A_s f'^{0.30}_c E^{0.44}_c \quad (1)$$

However, the simplified equation given below was suggested and accepted for use in design (i.e., see AISC Manual of Steel Construction (Load and Resistance Factor Design (1998), AASHTO Standard Specifications for Highway Bridges (1996), and AASHTO LRFD Bridge Design Specifications (1998)).

$$Q_u = 0.5 A_s \sqrt{f'_c E_c} \le F_u A_s. \quad (2)$$

Use of Equation 2 for some combinations of parameters may produce predicted capacities greater than the product of the cross-sectional area of the stud and the ultimate tensile strength of the stud (F_u). Therefore, the ultimate capacity in Equation (2) was limited to this value. Correlation of the test data to these two equations is shown in Fig. 2.11.

2.5.2 Influence of Stay in Place Metal Decking

Grant et al. (1977) furthered the previous research by investigating how the shear capacity of the studs was influenced by the use of steel decks. In this study, beam tests were used to evaluate the performance of composite beams using formed steel decks of varying geometry with ribs oriented perpendicular to the beam. As a result, a stud

reduction factor (SRF) to be applied to the above equation (when formed steel deck oriented perpendicular to the beam is used) was proposed and is used in the AISC Manual of Steel Construction (LRFD),

$$SRF = \frac{0.85}{\sqrt{N_r}}\left(\frac{w_r}{h_r}\right)\left(\frac{H_s}{h_r} - 1.0\right) \leq 1.0 \qquad (3)$$

where N_r = number of studs per rib

w_r = average width of concrete rib

h_r = rib height

H_s = height of shear stud after welding.

Later studies by several researchers (Hawkins and Mitchell, 1984; Jayas and Hosain, 1988 and 1989; Robinson, 1988; Mottram and Johnson, 1988; Lloyd and Wright, 1990) have shown that the strength predicted for studs used in conjunction with stay in place metal decking using Equations 2 and 3 is not conservative in some situations.

As a result, research by Easterling et al. (1993) sought to resolve this discrepancy. After a thorough review of past data, they hypothesized two possible reasons for the disparity between calculated and experimental results in some situations. First, the majority of the specimens tested by Grant et al. used composite beams where studs were arranged in pairs. Situations such that there is only one stud per rib may provide less strength than calculations predict. Secondly, the types of deck used by Grant et al. did not have a stiffener in the bottom flange as is typical of most deck profiles manufactured in the United States. When decks that do have these stiffeners are used, the studs must be welded off center, which may also affect the strength of the stud. Experimental testing was then performed to determine what effects, if any, these two variables caused.

Push-out tests with only one shear stud per rib were performed to determine the effects of placing the studs off center. Specimens with studs in the "weak" position and specimens with studs in the "strong" position were tested and compared. A stud that is placed on the side of the stiffener nearest the end of the beam is termed to be in the strong position, while a stud located on the side of the stiffener nearest the location of maximum moment is in the weak position (Fig. 2.12). The testing program also included beam tests using beams with only one shear stud per rib. The results of this testing again confirmed that the current equations over-predict the shear strength of the connection and subsequently the moment capacity of the composite beam when only single studs are used. The beam test results also show that the actual strength of the connection is 66% of the predicted capacity when single studs are located in the strong position but only 59% when single studs are placed in the weak position.

As a result, Easterling et al. offered the following design recommendations. First, they believe the current equations are conservative for cases when two or more studs are used and recommend no changes for this situation. However, when only single studs are used they recommend limiting the stud reduction factor (Equation 3) to a maximum of 0.75. Secondly, they suggest that all studs used in conjunction with formed metal deck having stiffeners should be detailed in the strong position. They also suggest that future research should focus on determining a strength reduction factor, ϕ, to be used in this situation.

Unrelated research by Oehlers and Johnson (1987) focused on modifying the work of Ollgaard et al. to account for the number of studs per span. This was of interest because the authors believe there is an increase in the probability of failure at a given

load per stud as the number of studs in a span reduces. In addition, the effects of using variable tensile strength (F_u) and modulus of elasticity (E_s) of shear studs were investigated. After an analysis of the results from 110 push-out tests previously performed in other studies, the following equation was determined to predict the shear strength of stud connections

$$Q_u = KA_s(E_c / E_s)^{0.40} f'^{0.35}_c F_u^{0.65}, \quad (4)$$

where K is a factor to account for the number of studs subjected to similar displacements (n) and is expressed as

$$K = 4.1 - n^{-0.5}. \quad (5)$$

2.6 Fatigue Resistance of Shear Studs

Current fatigue design methodology, in the United States, for shear connectors (e.g., see AASHTO Standard Specifications for Highway Bridges (1996), and AASHTO LRFD Bridge Design Specifications (1998)) is a result of the work of Slutter and Fisher (1966). The test program consisted of push-out tests and investigated the effects of stud diameter, maximum stress, stress range, and compressive strength of concrete. Results showed that the maximum stress and the compressive strength of concrete had little effect on the fatigue strength of the connectors and that stress range was the most important variable.

Figure 2.4 shows a comparison of beam test and push-out test data from previous similar studies (King et al., 1965; Toprac, 1965). Since the lower limit of dispersion of the beam tests and upper limit of dispersion of the push-out tests overlap, as discussed

previously, it was deduced that the push-out tests gave a lower bound of connector failure and thus the results from the push-out tests were used to make design recommendations.

Figure 2.13 illustrates the relationship between stress range and number of cycles to failure for tests with ¾" studs (⅞" studs yielded similar results) at various levels of minimum stress. Regression analysis of the test data for both ¾" and ⅞" produced an expression for the number of cycles to fatigue failure (N) in terms of the stress range the connectors were subjected to (S_r),

$$\log N = 8.072 - 0.1753\ S_r \qquad (6)$$

where S_r is expressed in ksi. Additionally, an expression for the allowable range of shear stress (Z_r) for an individual connector was suggested,

$$Z_r = \alpha\, d^2 \qquad (7)$$

where d = the diameter of the stud in inches

α = 13,800 for a design life of 100,000 cycles

10,600 for a design life of 500,000 cycles

7,850 for a design life of 2,000,000 cycles.

These recommendations were accepted by and are still contained in the AASHTO Standard Specifications (1994). The AASHTO LRFD Specifications also incorporate the above equations with a few modifications. The primary change between the allowable shear stress recommended by Slutter and Fisher and that used in the AASHTO LRFD code is that α is no longer a constant based solely on the design life and is instead expressed as

$$\alpha = 238 - 29.5 \log N, \qquad (8)$$

where N is a function of the annual daily truck traffic (ADTT) of the bridge, bridge geometry, and the location of the stud along the span.

Assuming complete interaction, the horizontal shear to be transferred by the shear connectors is expressed as

$$H = \frac{VQ}{I}, \tag{9}$$

where H = horizontal shear stress per inch of length

V = shear force

Q = moment of area of the transformed compressive area of concrete about the neutral axis of the composite section

I = moment of inertia of the composite section.

If range of shear force (V_r) is substituted for shear force, the result will be the range of horizontal force (H_r) that the connection must resist. Finally, Slutter and Fisher recommended the spacing of shear connectors (p) should be

$$p = \frac{nZ_r}{H_r}, \tag{10}$$

where n is the number of connectors. This recommendation is also used in both the AASHTO Standard Specifications (1996) and AASHTO LRFD Specifications (1998).

2.7 Combined Approach to Shear Connector Capacity

Recent research by Oehlers (1990) has proposed an alternative design method where static strength and fatigue resistance are integrated. Experimental testing of specimens subjected to fatigue loading and then statically loaded until failure shows

decreasing static strength due to an increasing number of cycles of fatigue loading (Fig. 2.14). This indicates that the static strength of shear connectors decreases as fatigue loads are applied. Therefore, it is Oehlers' opinion that current design practices, which account for fatigue resistance and static strength separately, do not accurately simulate the actual behavior of the shear connection.

Oehlers suggests an alternative method of shear connector design. This approach requires the initial static strength of the connection (P_s) to be greater than that required to resist the maximum design load (P_m). However, fatigue loads reduce the static strength to P_m at the end of the design life. The following iterative equation is proposed to determine the initial static strength of a connection (P_s) required

$$\frac{R_1}{P_s} = \left[\frac{10^K \left(1 - \frac{P_m}{P_s}\right)}{Cn_t + Cn_t \left(\frac{R_2}{R_1}\right)^m + \ldots + Cn_t \left(\frac{R_r}{R_1}\right)^m} \right]^{1/m}, \qquad (11a)$$

where R_i = a range of shear load induced by the standard fatigue vehicle (Fig. 2.15)

r = number of ranges of cyclic load

$$K = 2.68 - \frac{0.704}{\sqrt{n}} \qquad (11b)$$

n = number of connectors subjected to similar displacements

$$P_s = k f_u A \left(\frac{E_c}{E_s}\right)^{0.40} \left(\frac{f_{cu}}{f_u}\right)^{0.35} \qquad (11c)$$

$$k = 4.1 - \frac{1.0}{\sqrt{n}} \qquad (11d)$$

f_u = tensile strength of the stud material

A = cross-sectional area of the stud

E_c = modulus of elasticity of concrete

E_s = modulus of elasticity of stud material

f_{cu} = cube strength of concrete

m = -5.1 (constant determined from regression analysis of experimental data (Oehlers, 1995)

C = constant that is a function of the frequency and weight of the vehicles

n_t = number of fatigue cycles to which the structure is subjected.

Using this method, the distribution of shear connectors required to resist the maximum design load is determined first and then the density of this distribution is increased to allow for damage during the design life.

2.8 Discussion of Current FRP Deck to Steel Girder Connections

Various FRP deck manufacturers have developed proprietary type connections for use with their respective products and these have been implemented with varying degrees of success. For practical purposes, these connections can be divided into three categories: stud type connections, clamped connections, and bolted connections. Additionally in some instances manufactures have used adhesives in an attempt to develop additional bond strength and to develop some percentage of composite action. This section describes several of the most prevalent existing connections.

2.8.1 Shear Stud Connections

Creative Pultrusions, Inc., Martin Marietta Composites (MMC), and Hardcore Composites are three manufacturers of FRP bridge decks that have utilized shear stud type connections (Market Development Alliance, 2000 and Lesko, 2001). Creative Pultrusions, Inc. manufactures Superdeck™, a bridge deck formed by alternating double trapezoidal and hexagonal pultruded sections that are bonded together. Duraspan is a similar product manufactured by Martin Marietta Composites (MMC) composed of pultruded trapezoidal sections bonded together. Hardcore Composites manufactures honeycomb sandwich panels using an adaptation of Vacuum Assisted Resin Transfer Molding (VARTM).

The shear connection designed by Creative Pultrustions, Inc. for use with Superdeck™ (Fig. 2.16) begins with a 4" diameter hole drilled through the deck over a girder. Then a shear stud is field welded to the girder. The hole is blocked off with cardboard and then filled with non-shrink grout. The hole is then covered with a bonded FRP flatsheet.

MMC has developed three similar types of connections to be used with Duraspan decks. Similar to the Superdeck™ connection described above, a hole is drilled through the FRP deck above the girder. The hole is then blocked off with foam inserts and shear studs are field welded to the top flange. The Duraspan connections consist of either ¾ or $^{7}/_{8}$" shear studs with a wire spiral, placed in pairs. The hole is then filled with non-shrink grout and covered with a FRP overlay. The primary difference in the three types of connections used by MMC lies in the type of material used to support the deck above the

girder and form the haunch. The three types of material currently available are a polystyrene support, a light gage angle support, or a wood form with a plastic shim. These connections are similar to the connection shown in Fig. 2.16.

Hardcore Composites is a third company implementing a similar type of connection for use with their bridge deck. The connection consists of a shear stud fitted in a hole that has been drilled through the deck. As in other connections of this type, the hole is then filled with grout to secure the connection.

Shear stud connections, like those described above, provide for the transfer of forces between the deck and the girders while securing the deck in place and preventing uplift. Shear stud connections also provide ease in construction by utilizing shear stud methods that are familiar both to engineers and construction crews. However, the durability of the grout and the stud under fatigue loading, as well as the material used to contain the grout, are issues of concern.

2.8.2 Clamped Connections

Kansas Structural Composites, Inc. (KSCI) manufactures a FRP deck comprised of a top and bottom face sheet with a sinusoidal honeycomb type FRP core. They have adopted a clamp-type connection for the use of these panels in bridge applications (Meggers, 2000). The connections are placed at panel-to-panel joints. Each joint contains a FRP tube in which the connection is made. Holes are drilled through the tube and bolts are used to secure a clamping device against the FRP tube and the bottom of the steel girders top flange (see Fig. 2.17). This assembly will effectively prevent uplift of

the panels at the joints, although spacing the connections only at the ends of the panels may be too liberal to provide adequate restraint. The clamp device is also fairly labor intensive, as the connection needs to be installed from underneath the bridge deck.

2.8.3 Bolted Connections

Bolted connections are the third category of connections currently used with FRP bridge decks. Often blind bolts are used in conjunction with one of the other types of connections discussed above. Blind bolts are similar to traditional bolts except that the head of the bolt is replaced by a small flat plate with the ability to rotate. The blind bolts are installed from underneath the bridge deck through holes that have been drilled through the top flange of the girder and the bottom of the FRP deck. Blind bolts are an effective way to secure the deck in place and prevent uplift and rotation. However, the installation process is quite labor intensive, because the work must be performed from underneath the bridge deck and also due to the of the relatively close spacing of blind bolts (typically 12-24 in.). Additionally, as the critical components of the bolt are inside of the bridge deck, there are problems involved with inspection. There may also be fatigue concerns with these connections.

Occasionally, traditional bolts are used to provide a connection between FRP decks and girders (Lesko, 2001). These are typically installed inside of steel sleeves through matched holes drilled through the entire depth of the deck and the top flange of the girder (see Fig. 2.18). These adequately restrain the deck, as well as prevent uplift and rotation.

Similar to blind bolts, these also require installation from underneath the surface of the deck. Additionally, loosening of the nut under fatigue loading may be a concern.

2.9 Summary

Throughout the past several years, researchers have sought to reliably and accurately predict the static strength and fatigue resistance of shear studs. Typically this has involved experimental testing using a combination of push-out and beam specimens. As a result of this research, parameters affecting the strength and performance of shear studs have been determined and design equations have been developed.

Because the connection between FRP bridge decks and steel girders has not been thoroughly investigated, this previous research on shear studs provides important information that is useful in the present study of a connection between FRP bridge decks and steel girders. Specifically, the information presented here on testing methods will be used to formulate a testing scheme for the proposed connection. In addition, an understanding of shear stud behavior provides valuable insight into the behavior of the proposed connection for FRP bridge decks.

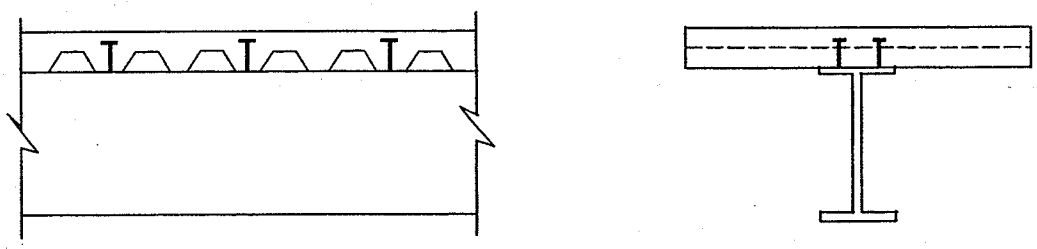

Figure 2.1: Typical Beam Test Specimen
Elevation View and Cross Section

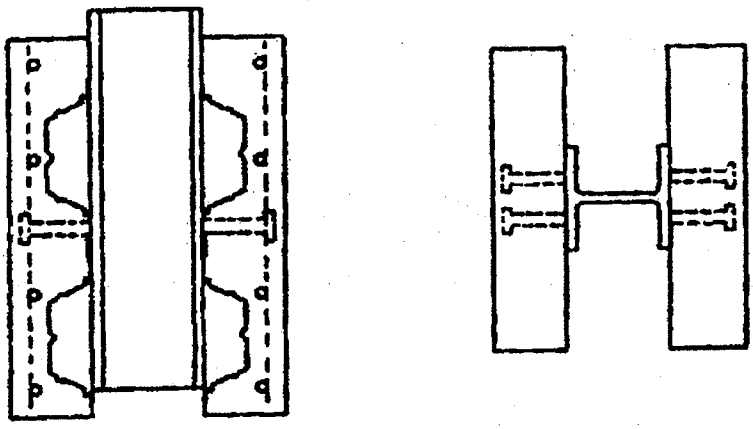

Figure 2.2: Typical Push-out Test Specimen (Type 1)
Elevation and Plan View

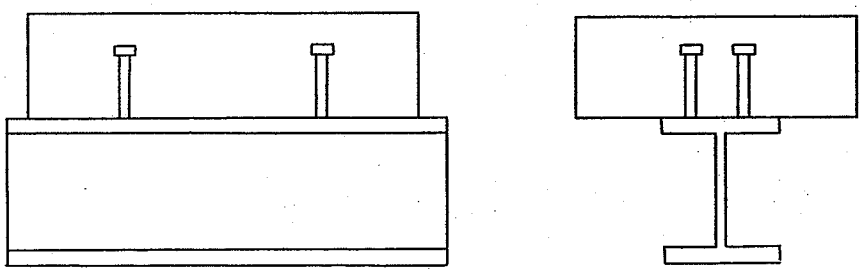

Figure 2.3: Typical Push-out Test Specimen (Type 2)
Elevation View and Cross Section

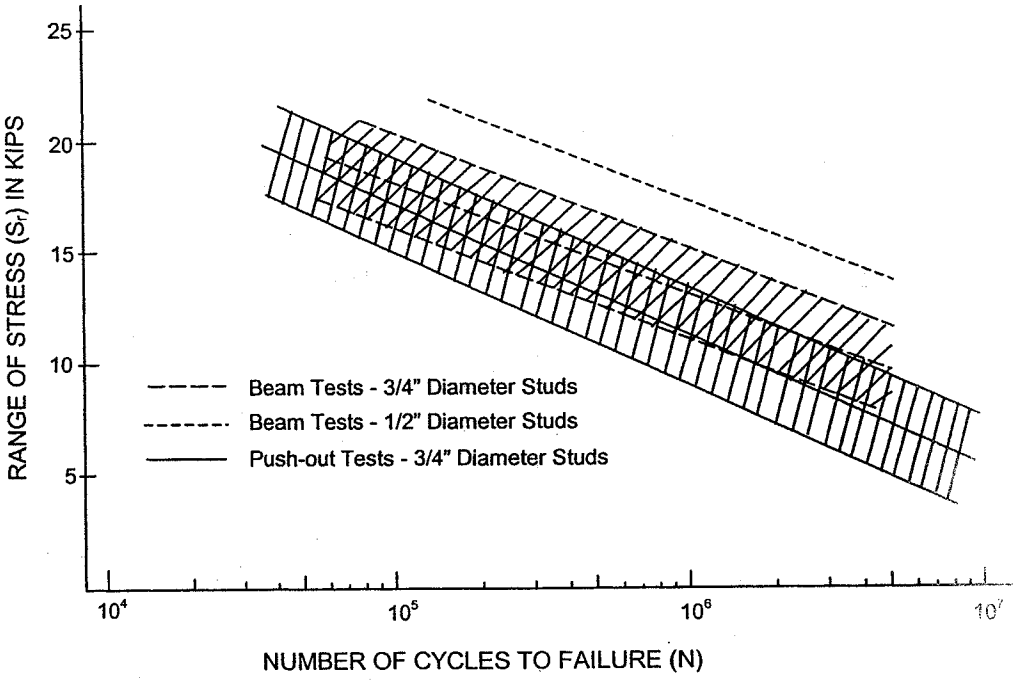

Figure 2.4 Comparison of Beam Tests and Push-out Tests
(Slutter and Fisher, 1966)

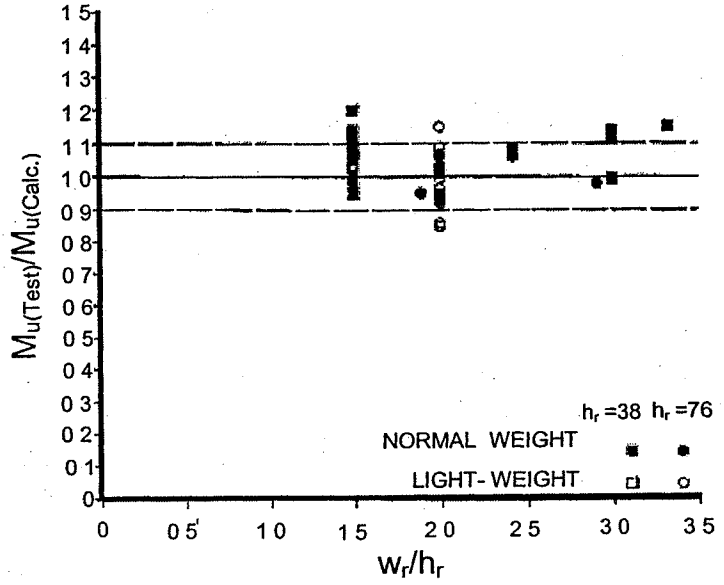

Figure 2.5: Comparison of Beam Tests and Push-out Tests
(Jayas and Hosain, 1989)

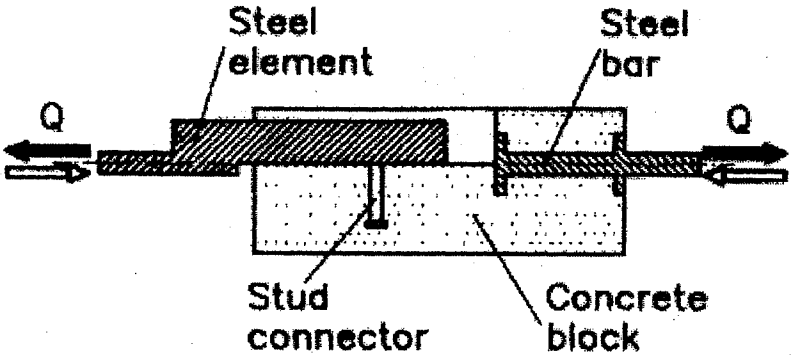

Figure 2.6: Direct Shear Test Configuration

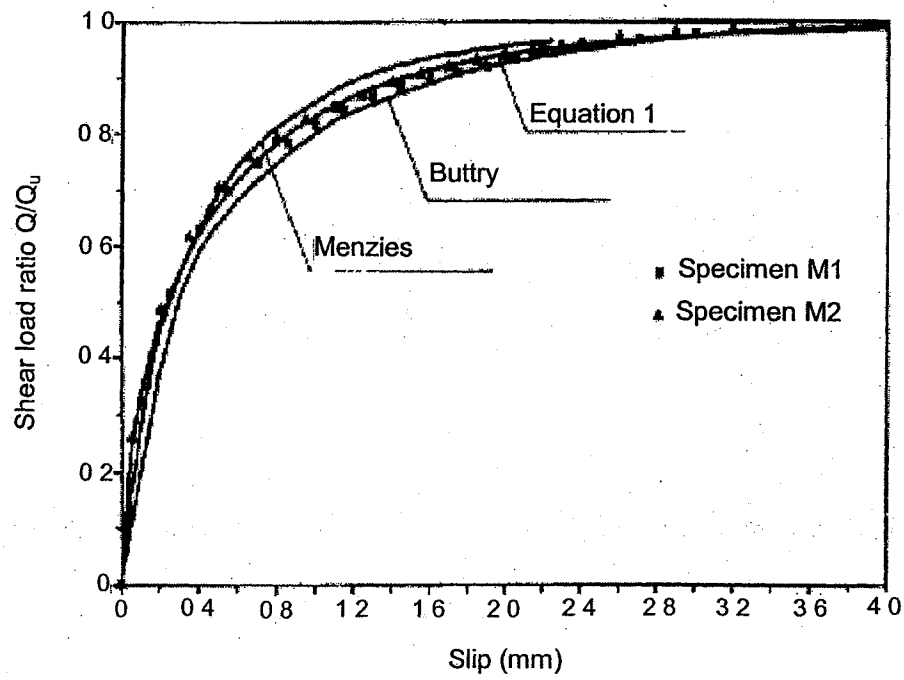

Figure 2.7: Comparison of Direct Shear and Push-out Tests

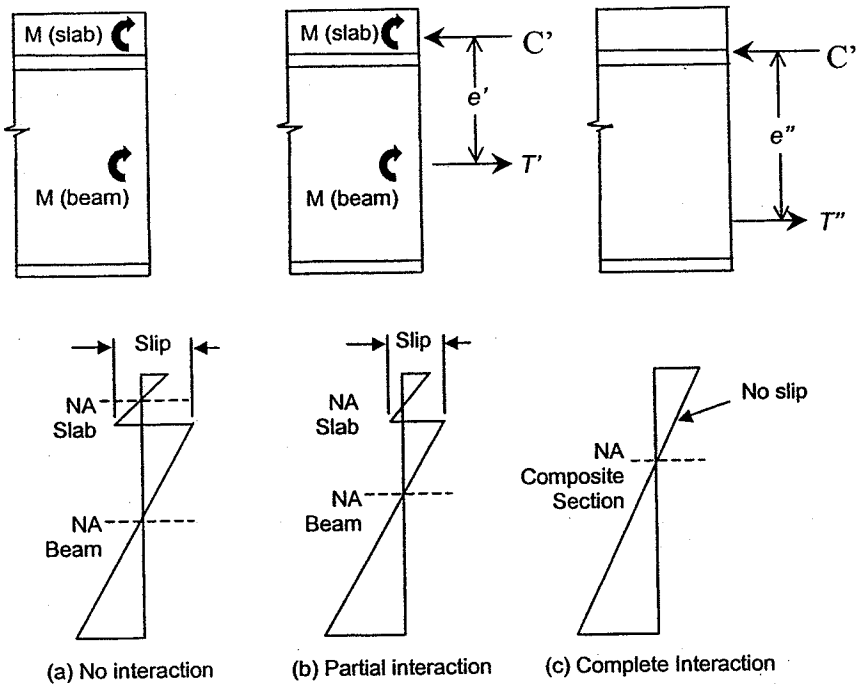

Figure 2.8: Forces and Strain Variation at Different Levels of Composite Action

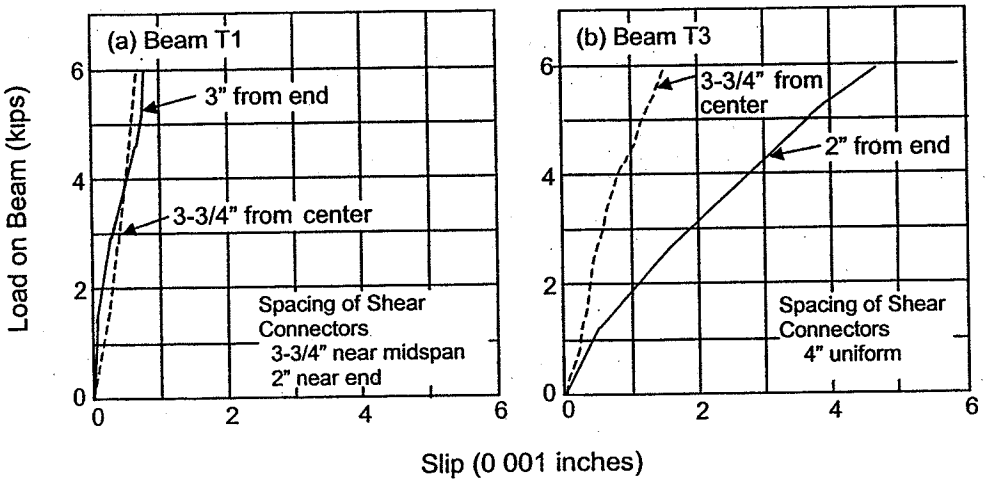

Figure 2.9: Comparison of Variable vs. Uniform Spacing of Connectors

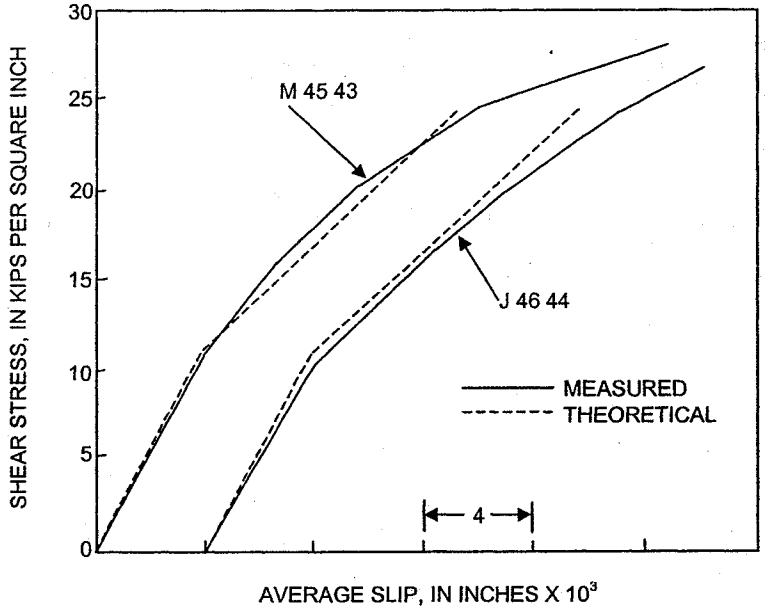

Figure 2.10: Comparison of Measured and Theoretical Shear Stress Approximating Stud Behavior as an Elastic Dowel on an Elastic Foundation

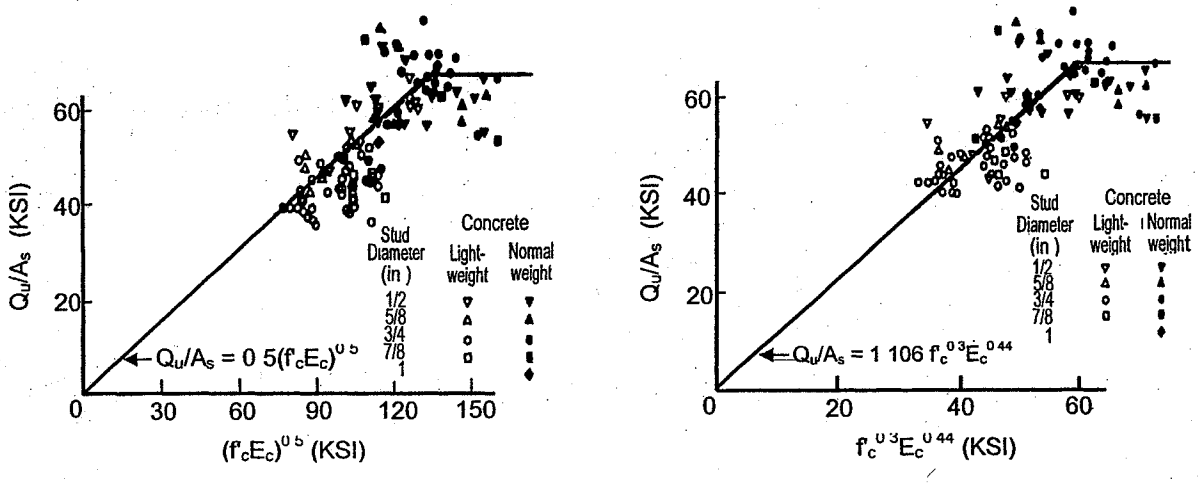

Figure 2.11: Correlation of Test Data to Strength Equations Suggested by Ollgaard, Slutter, and Fisher

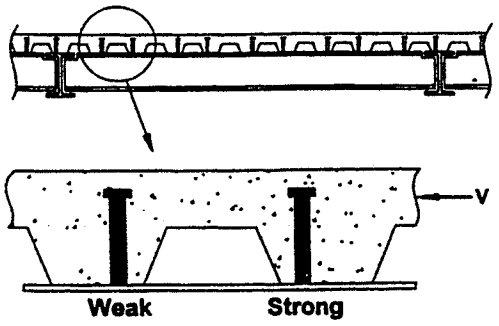

Figure 2.12: Strong and Weak Position Shear Studs

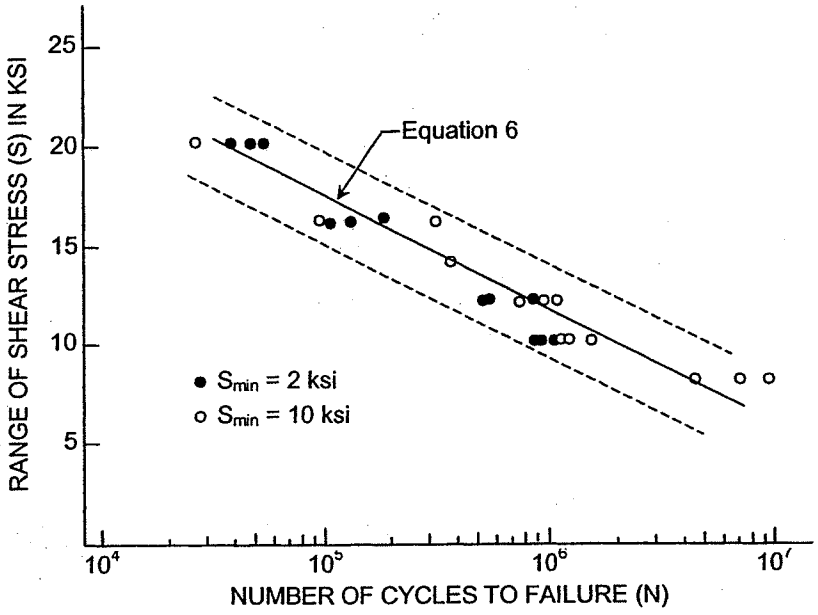

Figure 2.13: Stress Range vs. Number of Cycles to Failure
For ¾" Diameter Studs

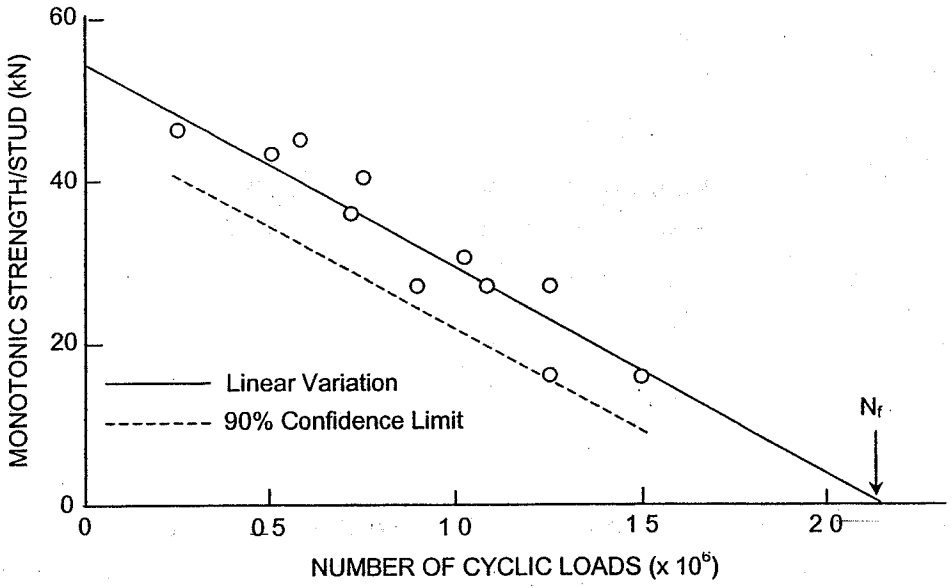

Figure 2.14: Comparison of Static Strength of Shear Studs vs. Number of Fatigue Cycles Applied

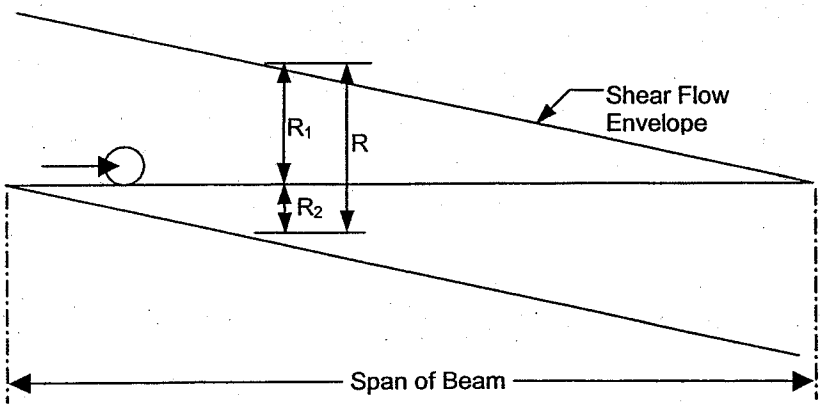

Figure 2.15: Range of Shear due to Moving Point Load

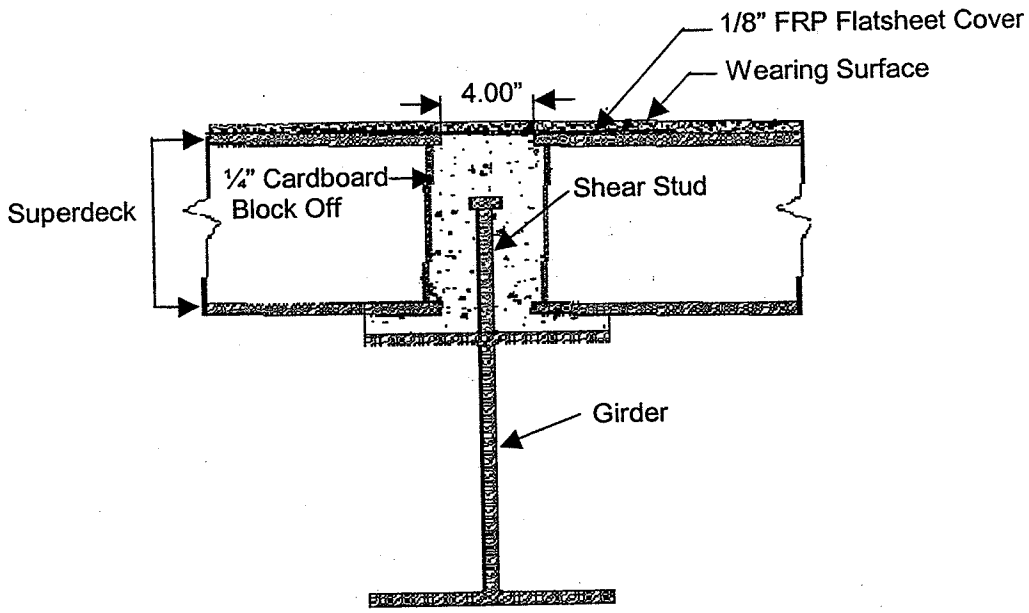

Figure 2.16: Superdeck™ Shear Stud Connection

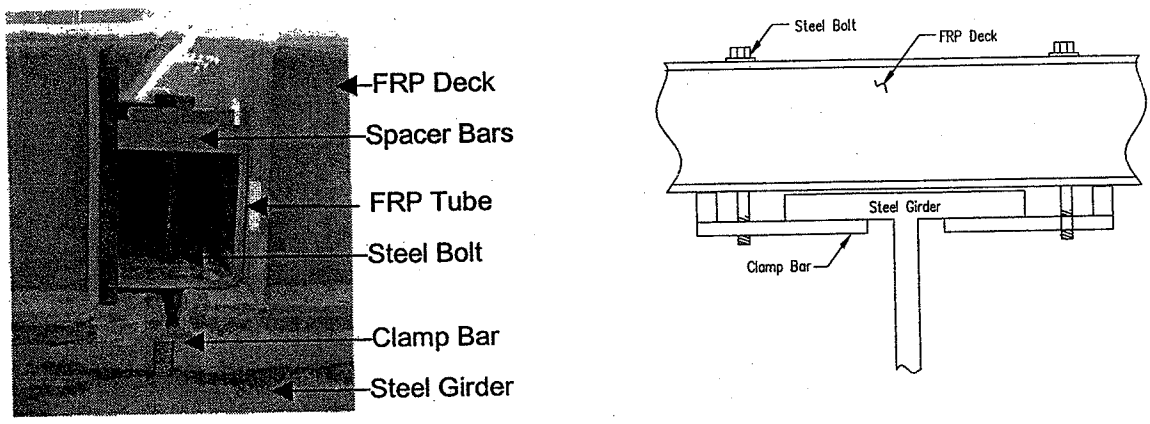

(a) Elevation View

(b) Cross Section

Figure 2.17: KSCI Clamp Connection and Girder

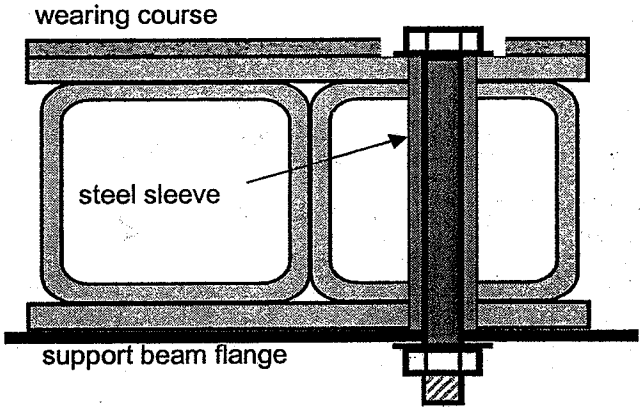

Figure 2.18: Bolted Connection

Chapter 3

CONNECTION DESIGN

3.1 Conceptual Development

The first task of the current study was to develop a simple, efficient and economical connector for use with FRP decks in conjunction with steel bridge girders. After studying the performance and installation issues of various existing connections, it was decided that a welded shear stud type connection that could provide a positive clamping force to the deck would be the most efficient design. As a result, the connection shown in Fig. 3.1 was developed.

As shown, this connection consists of a threaded shear stud welded to the top flange of the supporting girder and housed inside of steel sleeves that are installed within a hole drilled through the FRP deck. The steel sleeves are sized such that the inner jacket of the top sleeve fits inside of the bottom sleeve. In addition, the top sleeve is fabricated with a fixed inner washer near mid-height that provides bearing area to tighten a nut against and a second top washer acts to clamp the deck in place as the nut is tightened.

As the goal of this task was to provide an efficient alternative to current connection methods, it was important that the new connection design addressed several criteria. Those criteria considered during the design of this connection were: prevention

of uplift, versatility, ease in installation, cost effectiveness, ease in replacement, and structural efficiency.

The proposed design provides a secure connection, preventing uplift of the bridge deck by way of the top washer of the steel sleeve, i.e., as the nut is tightened, the top washer exerts a downward force on the FRP deck. Another important feature is that this connection has the ability to be used in conjunction with any type of commercially available FRP bridge deck, including pultruded and sandwich decks. In addition, the height of the sleeves can easily be adjusted, creating a functional connection for various deck thicknesses.

Implementing familiar shear stud technology and having the potential of pre-installation of the steel sleeves by the FRP manufacturer enable the design to be both easy to install and cost effective. Construction of this connection would involve: welding the threaded studs to the girder (similar to what is done in the construction of reinforced concrete bridge decks), placing the FRP deck with the sleeves installed, placing and tightening the nuts on the stud to secure the deck, and then covering the sleeves in some manner, perhaps a FRP overlay or cap made to fit inside the top sleeve. Allowing all labor to be performed from above the bridge deck further facilitates ease in installation. This would significantly expedited placement procedures compared to some of the current connection methods for FRP bridge decks. As a result, construction time could be reduced, providing some cost savings. Considering the cost of materials alone, the estimated cost of these connections is under $100 per connection. This includes the price of the sleeves, stud, and nut.

In the event there is a need for replacement of the deck, the connection could easily be replaced by removing the nut and washer. An additional attribute of this connection is its structural efficiency. Since composite materials have relatively low compressive and shear strength properties, this connector minimizes these stresses by way of the protective steel sleeves and relatively large contact surface area provided by the oversized hole. Additionally, the favorable fatigue performance of steel shear studs is well established.

3.2 Finite Element Analysis of Proposed Connection

Once the concept for this connection was developed, finite element analysis (FEA) was used to aid in the selection of appropriate dimensions for use in the development of a prototype. Specifically, information regarding appropriate hole/sleeve diameter and top washer diameter was desired. This section summarizes the finite element analysis performed for this purpose at the University of Akron by Dr. Pizhong Qiao and X. Frank Xu and is provided here in order to present a complete discussion of the development of this connection.

3.2.1 Formulation of Finite Element Model

Finite element analysis of this connection was accomplished by using the commercial finite element program ANSYS 5.5. The deck was modeled using the characteristics and material properties of honeycomb FRP panels produced by Kansas

Structural Composites, Inc. (KSCI) since the same panels would be used in the experimental testing. The reader is referred to "Modeling and characterization of fiber-reinforced plastic honeycomb sandwich panels for bridge applications" by Davalos, et al. (2001) for additional information on these panels.

To determine the appropriate dimensions to use for the FRP panel in the model, the ratios of laminate width to hole diameter (w/d) and end distance to hole diameter (e/d) were evaluated. It was found that the ultimate strength of the connection becomes nearly constant once these ratios are above a certain value. Therefore, the next task was to obtain these limiting ratios. Because from a structural point of view, bearing failure is the most desirable failure mode (Ramakrishna et al., 1999), it was desirable to provide the necessary geometry to suppress the tensile and shear modes of failure. A review of current literature showed that bearing failure occurred when $w/d > 6$ and $e/d > 4$ for highly orthotropic laminae (Wang et al., 1998). Based on this information, ratios of $w/d = 6$ and $e/d = 6$ were used in the FEA model. A comparative study was conducted to check the sufficiency of these limits to ensure the bearing mode of failure.

The connection was modeled as a single bolted hole with the connection components (stud, washer, nut, and sleeves) represented as one rigid unit and the interaction between the bolt and the edge of the hole was modeled using contact elements. Furthermore, it was assumed that there is no clearance between the hole and the bolt, even though in reality there is a void between the stud and sleeves.

The interaction between the bolt and the hole was simulated by applying a uniform axial stress at the remote end of the hole while holding the bolt fixed. At the hole boundary on the loaded side of the bolt, the displacements parallel to the stress were

assumed to be zero. The model was divided into two meshing regions, a fine mesh region in the vicinity of the hole and a coarser mesh elsewhere.

It was decided the hole diameter should be as small as practically possible as previous studies have shown that strength decreases with increasing hole size (Waddoups et al., 1971). With using a 7/8 in. diameter threaded stud, it was thought that the minimum hole size possible would be approximately 1.5 in., (7/8 in. plus a minimum clearance of 0.3 in. on each side). For this study the results due to a 1.5 in. and a 2 in. diameter hole were compared. Conversely, it was believed the washer diameter should be as large as practical since clamping pressure exerted by the washer will increase the strength of the connection. Consequently, results due to washer diameters of 2 in., 3 in., and 4 in. were evaluated.

3.2.2 Analyses of Model and Results

Two analyses were conducted in this study corresponding to the two primary loads acting on the connection: a shear/bearing force and a bending moment. The effects of varying the diameter of the hole were investigated in the bearing study, while the effects of varying the washer diameter are examined in the bending study.

For a sandwich deck with an applied shear force, it can be assumed that the two face laminates equally resist this force and that the core of the deck does not contribute to the shear strength of the panel. This enabled the bearing study analysis to be simplified to a two-dimensional model consisting of only one face sheet and the connection. For

this study, the laminate was modeled with 8-node isoparametric shell elements and the 20 layers of the face sheet (see Davalos et al., 2001) were defined.

Also, for the bearing analysis, the transverse clamping force applied by the washers to the face laminates, as well as friction between the bolt and the laminate were neglected. This led to more conservative results since both of these factors would increase the strength of the connection. Furthermore, laminate delamination was not considered due to the complexity of this mode of failure. This was justified by Qiao and Xu by asserting that the laminate bearing strength will be increased and delamination minimized by use of the steel sleeves.

For the bending mode study, the effects of bending moment were simplified as a tensile force on the bottom face and a compressive force on the top face. Thus for this analysis, the sandwich panel was modeled as an equivalent 3-layer laminate consisting of the top face laminate, core, and bottom face laminate where the multiple layers of the face laminates are represented as a single orthotropic layer. The clamping force exerted by the washers is accounted for in this analysis by imposing zero lateral displacements on all the nodes within the contact area of the washer. As in the bearing mode study, the effects of friction between the bolt and the laminate and laminate delamination are not considered.

From the FEA two conclusions were provided. First, results of the bearing mode study found that a smaller diameter hole provides a more efficient joint as the bearing stress concentration factor (k_b) of the 1.5 in. diameter hole is smaller than the factor for the 2.0 in. diameter hole (Fig. 3.2). Secondly, the bending study showed that there was an insignificant difference in the strength of the connection as a result of various washer

diameters with only a 5% difference in strength when the washer diameter doubled from 2 in. to 4 in.

3.3 Selected Dimensions

Considering the FEA results, dimensions for a prototype connection were selected. While the results from the finite element analysis indicate that the ideal hole diameter was 1.5 in., this was not possible due to constructibility issues. It was required that the hole diameter be increased to allow for tightening clearance of the nut. For a $^{7}/_{8}$ in. diameter bolt, a 2.5 in. socket clearance is required (see American Institute of Steel Construction (AISC), 1994). As a result, the inside diameter of the sleeve was selected to be 2.75 in. to allow for ease in construction. In addition, a $^{1}/_{8}$ in. wall thickness for the sleeves was selected, resulting in a required hole diameter of 3 in. Since results from the FEA show that washer diameter did not play a significant role in connection strength, a relatively small washer (extending only 1 in. beyond the hole) was selected.

The remaining dimensions of the initial connector were determined based on practicality and engineering judgement. The prototype connector is subsequently tested using a 5 in. deep sandwich panel. Therefore, the vertical dimensions were selected to work well with this depth of panel. However, it should be noted that the sleeve configuration could be altered to allow for considerable adjustment of vertical dimensions, accommodating use over a wide range of deck thickness. Figure 3.3 shows the dimensions selected for the sleeves used in the prototype connections. In addition, stainless steel was chosen to be the material for the sleeves in order to minimize

corrosion. Thus, the prototype connections were manufactured from 11L17, which is a stainless steel alloy.

3.4 Conclusion

In summary, a shear stud type connection involving the use of protective steel sleeves was designed and manufactured. The use of finite element analysis was employed to aid in the selection of appropriate dimensions for the connections. Figures 3.1 and 3.3 show the proposed connection and dimensions used, respectively. Subsequent chapters describe experimental and analytical studies focused on evaluating the performance characteristics of this initial connection design.

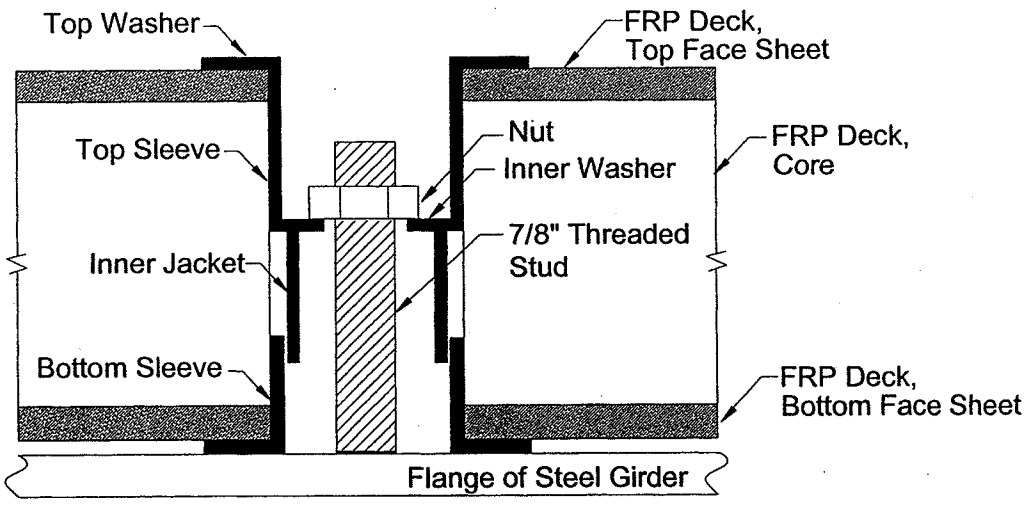

Figure 3.1: Proposed Connection for FRP Decks to Steel Girders

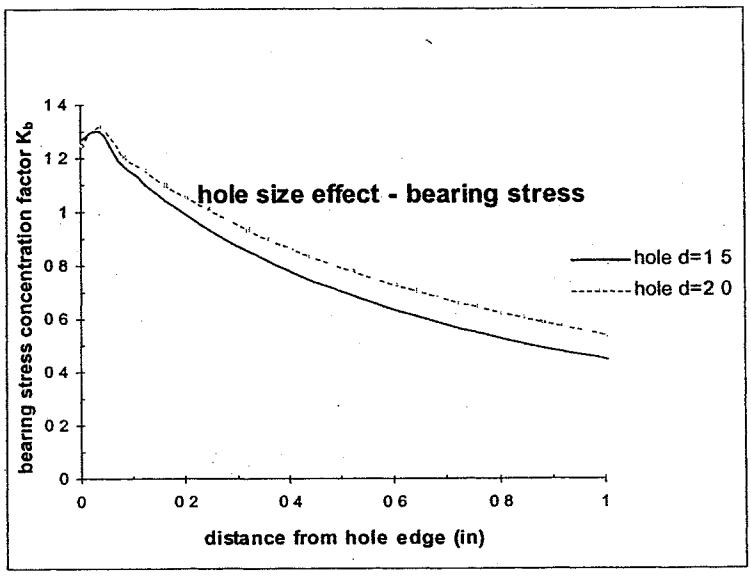

Figure 3.2: Bearing Stress Concentration Factor, kb

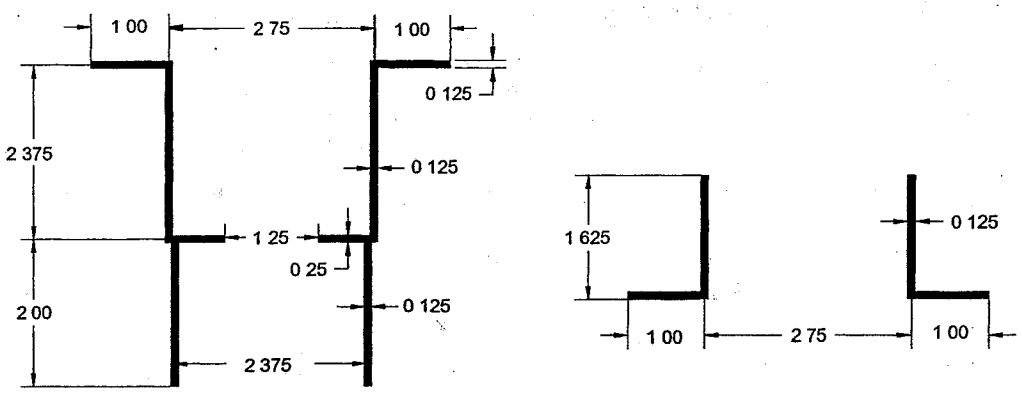

Figure 3.3: Sleeve Dimensions (Inches) Used in Prototype Connections

Chapter 4

INDIVIDUAL CONNECTOR STRENGTH

4.1 Introduction

This section describes initial experimental testing focused on determination of the static shear strength of individual connections. Tests were performed on the connection described in Chapter 3, as well as three modified versions, including one fully grouted connection. A description of the various connection designs investigated, the procedure used to determine the strength of an individual connection, and results of this study are provided in this chapter.

4.2 Connection Designs Investigated

The three different types of sleeve configurations used in the test specimens are shown in Figs. 4.1 through 4.3. Figure 4.1 shows the connection originally developed, as discussed in Chapter 3, which is referred to as Type 1 connection. The connection shown in Fig. 4.2, referred to as Type 2 connection, is the same as the Type 1 connection with the exception that the top sleeve does not have an inner jacket that fits inside of the bottom sleeve. Figure 4.3 shows the Type 3 connection, which contains only a top sleeve with no inner jacket. A fourth alternative, consisting of the Type 1 connector with the void inside the sleeves filled with high-strength epoxy grout, was also tested.

Grouted specimens used Masterflow 648 CP Plus epoxy grout (manufactured by Master Builder Technologies). This was mixed using a fill ratio of 5.06; that is, the mass of aggregate used was 5.06 times the mass of the liquid components. This is the minimum fill ratio recommended by the manufacturer and was chosen so that the grout would flow easily through the inner washer of the top sleeve. However, even using this low fill ratio, the grout was not fluid enough to easily pass through the gap between the stud and the inner washer, making the process somewhat labor intensive. The specimens were allowed to cure for a minimum of seven days before loading, at which time the minimum compressive strength of the grout (per the manufacturers specifications) is 11,500 psi. No tests were performed to verify the properties of the grout.

4.3 Test Setup and Procedure

Figure 4.4 shows the basic test setup used for assessing the static shear strength of individual connectors. Each test consisted of bolting a $^1/_2$ in. thick steel plate to the flange of a W12 x 120 steel column. Also, a single $^7/_8$ in. diameter threaded steel stud was welded to the face of these plates using a stud gun (see Fig 4.5). This method provided for both accurately simulating the condition of a shear stud welded to a bridge girder and efficiently performing multiple tests.

The test specimens consisted of 12 in. x 12 in. sections of 5 in. deep honeycomb sandwich panels manufactured by Kansas Structural Composites, Inc. The steel sleeves were installed in a 3 in. diameter hole drilled in the center of the panels. The panel and

sleeve assembly was then bolted to the shear stud on the steel plate using a nut and washer.

The specimen was loaded using a hydraulic ram and a load cell was used to record the applied load at regular intervals. An aluminum bracket was tightened surrounding the FRP specimen to help distribute the applied force more uniformly. Displacement data was recorded using two linear variable differential transformers (LVDTs), one placed on each side of the specimen. The core of the LVDTs was connected to the aluminum bracket using threaded rods (see Fig. 4.4).

Initial tests, focused on determining ultimate loads, involved loading the specimens at a constant rate until failure. Further tests, focused on assessing the level of damage incurred by the specimens at various load magnitudes, were later conducted. In these tests, the specimen was loaded and unloaded at increasing levels. At the end of given loading cycles, the specimen was unloaded and then disassembled. Each component (stud, sleeves, and panel) was then examined to determine the level of damage that had occurred at the given level of force. The connection was then reassembled and subjected to an increased force level. This process was repeated numerous times until failure of the specimen occurred.

4.4 Results

4.4.1 Ultimate Load Tests

The four types of connections discussed above were tested to failure and the differences in strength and overall performance were evaluated in this phase of testing.

From these tests, information was obtained regarding: the ultimate shear strength and mode of failure of the connection, the type and level of damage sustained by the components of the specimen, and the load versus displacement behavior of the specimens. The following tests were performed, loading the specimen continuously until failure:

- Three specimens with the Type 1 connection (Specimens O1, O2, and O3),
- Three specimens with the Type 2 connection (Specimens M1, M2, and M3),
- Three specimens with the Type 3 connection (Specimens R1, R2, and R3), and
- Two specimens using the Type 1 connection where the void inside the sleeves was filled with high-strength epoxy grout (Specimens G1 and G2).

It is noteworthy to mention that in addition to these eleven tests an additional test was performed that is not reported in the results. During loading of this specimen, the top face sheet of the panel completely delaminated from the core at a very low level of load. This was deemed to be the result of a manufacturing flaw in the panel, as this mode of failure was not observed in any of the other specimens.

Ultimate Strength:

The maximum strength obtained from the ultimate load tests is presented in Table 4.1. In summary, the maximum strength of the specimens with the Type 1 connection ranged from 31,700 to 37,300 lbs; the Type 2 connections developed maximum strengths

ranging from 31,200 to 33,400 lbs; the Type 3 connection exhibited maximum strength values ranging from 14,500 to 20,000 lbs; and the two grouted connections, G1 and G2, failed at 33,200 and 31,500 lbs respectively. In all of these tests, with the exception of the grouted specimens, failure was not due to a failure of the connection; instead, excessive damage to the FRP panel prevented the specimens from resisting any additional force. In the grouted connections, failure was due to fracture of the stud.

General Connection Performance:

In addition to assessing the static strength of the connection, the components of each specimen were inspected after loading in order to determine the type of damage that resulted to each component of the connection and the relative amount of damage incurred when using the different types of connections. As expected from the differing failure modes, the damage to the specimens without grout was distinctly different from the damage that was caused to the two grouted specimens. The following are comments characteristic of all the specimens tested without grout.

- There was substantial deformation of the stud (approximately 1" in most cases, see Fig. 4.6) accompanied by deformation of the threads of the stud near the location of the inner washer of the top sleeve (Fig. 4.7).
- The top sleeve experienced two types of damage: (1) warping of the top washer (see Fig 4.8) and (2) ovalization of the hole in the inner washer (see Fig. 4.9). In all cases, warping of the top washer occurred on the side of the washer closest to the applied load. This resulted from a slight load

eccentricity that tended to rotate the top of the specimen away from the column face.

- In specimens that incorporated a bottom sleeve, this sleeve became ovalized and exhibited an impression of the stud weld profile on the inside of the sleeve nearest the applied load (see Fig. 4.10).
- The bottom face sheets of the FRP panel became ovalized and discolorations surround the edge of the hole nearest the applied load, in some instances there is also some crushing of the face sheet in this location (see Fig. 4.11). The discolorations are a sign that stresses in the panel have caused a physical change to occur such as delamination or fiber failure. Note that the minor discoloration surrounding the entire hole is a result of hole drilling.

These observations led to the conclusion that during loading of these specimens the panel was sufficiently displaced such that the sleeves were forced into contact with the stud. Specifically, the stud comes into contact with the sleeves in two locations in all specimens: (1) at the root of the stud and (2) at mid-height of the stud corresponding to the location of the inner washer of the top sleeve. In addition, some specimens also showed evidence of a third point of contact with the stud, at the bottom of the inner jacket, as indicated by deformation of both the threads and the sleeve at this location. Figure 4.12 shows the deformed shape of the specimen after loading.

For each sleeve configuration used, comparisons were made regarding the relative amount of damage that each component incurred. These will be discussed in terms of each component, as follows:

- Stud: All connections resulted in a similar amount of deformation of the stud (approximately 1" for all specimens), as shown in Fig. 4.7.
- Top Sleeve: As mentioned previously, the top sleeves experienced two types of damage, warping of the top washer and ovalization of the hole in the inner washer. Only minimal warping was observed in the top sleeves of the Type 1 and Type 2 connection (see Fig. 4.13), while more significant warping was noticed in the Type 3 connections (see Fig. 4.8). Note that while Fig. 4.13 illustrates only the warping of the Type 2 connection, a similar amount of warping was displayed in the Type 1 connections. The second type of damage to the top sleeves, ovalization of the hole in the inner washer, occurred evenly in each type of connection. Figure 4.9 shows a representative photograph of the ovalization of the inner washer described.
- Bottom Sleeve: The damage that occurred to the bottom sleeves incorporated in both the Type 1 and Type 2 connections was identical. All bottom sleeves are ovalized and show an impression of the weld collar of the stud as shown in Fig. 4.10.
- Top Face Sheet of Panel: Specimens with the Type 1 connection and Type 2 connection displayed only minimal discolorations on the top face sheet (Fig. 4.14). Conversely, the specimens with the Type 3 connection showed significant discolorations (Fig 4.15). These specimens that showed excessive damage to the top face sheet are the same as those where significant warping of the top washer occurred. Therefore, it is

believed that the warping of the top washer caused reduced contact area between the top washer and top face sheet, which then resulted in increased stress around the hole in the top face sheet, directly contributing to the significant damage to the top face sheet in the specimens containing the Type 3 connections.

- Bottom Face Sheet of Panel: Figures 4.16 through 4.18 show the bottom face sheet of a representative specimen after testing with a Type 1 connection, Type 2 connection, and Type 3 connection, respectively. As shown in the figures, the specimens with Type 1 connections displayed minimal discoloration on the bottom face sheet compared to the other specimens. The specimens with the Type 2 connection showed more severe discolorations and even some crushing of the face sheet was visible in two of the three specimens. Since the specimens with the Type 3 connection did not have bottom sleeves, the applied force was distributed over a smaller contact area (stud only versus sleeve). Therefore, the bottom face sheet is more severely damaged and the damage is confined to a smaller surface area.

For the two specimens with grout, the type of damage that occurred was distinctly different from that of the non-grouted specimens. In fact, the only damage that was observed in the specimens with grout was the fracture of the stud, which in both samples occurred at the base of the stud (see Fig. 4.19). There was no noticeable damage to the top or bottom sleeves. Further, while there was no visual appearance of damage to the

FRP panels, a significant amount of cracking was heard throughout the test, which is characteristic of delaminations/fiber failure occurring.

Load vs. Displacement Behavior:

Displacement data was recorded at regular intervals throughout each test. As mentioned previously, one LVDT was placed on each side of the specimen, which are referred to as "left LVDT" and "right LVDT" (see Fig. 4.4). While there was some discrepancy in left and right LVDT readings, which is attributable to small rotations of the specimen, load displacement results present averaged values that negate the influence of this specimen rotation.

Figure 4.20 shows the average load-deflection plot for all specimens tested. Note that the maximum loads reported in the graph do not necessarily correlate with the results presented in Table 4.1. This is because in some of the tests, the LVDTs were removed before the ultimate load was achieved to avoid damage to the instrumentation. Thus, the results in Fig. 4.20 are conservative in several cases.

Several observations regarding the load deflection data may be made:

- First, for the Type 1 and Type 2 connections there are two distinct slopes, i.e., up to approximately 10,000 lbs there is one slope and beyond 10,000 lbs there is a second, steeper slope. This phenomenon is not seen in the Type 3 connections. Also, the second, steeper slope of the Type 1 and Type 2 connections is approximately equal to the slope of the grouted connections.

- Second, this data reinforces the ultimate load data presented in Table 4.1 in that the performance of the Type 1 and Type 2 connections is far superior to that of the Type 3 connection, both in ultimate load sustained and decreased displacement at higher loads.
- Finally, the specimens with grout exhibit a much higher apparent stiffness than the other specimens tested.

In summary, as a result of the ultimate load testing phase of this research several conclusions were made. First, the ultimate strength obtained using the Type 1, Type 2, and grouted connections are all similar, though the Type 1 connections provide the greatest average strength. It was also determined that, when grout was not used, failure of the specimens was not due to a failure of the connection, but instead was a result of the inability of the FRP panel to withstand any additional force i.e., the initiation of a bearing failure in the FRP panel. Also, it was shown that even though the connection did not fail when using the Type 3 connection, the use of the bottom sleeve greatly enhanced the strength of the connection by distributing the applied forces over a larger contact area. While there may have been less displacement in the grouted samples, failure was considerably more catastrophic. Therefore, the Type 1 and Type 2 connections were the only connections studied in subsequent research.

4.4.2 Damage Evaluation Tests

The objective of this phase of testing was to determine the amount of damage incurred at various levels of load when using the Type 1 and Type 2 connections. The following tests were performed, subjecting the specimen to increasing amounts of load

throughout several cycles of loading and unloading as previously described:

- Two specimens with the Type 1 connection, where loading was increased in increments of approximately 5,000 lbs up to 25,000 lbs, then the specimen was loaded to failure (Specimens O4 and O5),
- One specimen with the Type 1 connection, where loading was increased in increments of approximately 500 lbs until the stud had yielded, then increments of approximately 5,000 lbs were used until failure occurred (Specimen O6), and
- Two specimens with the Type 2 connection, where loading was increased in increments of approximately 500 lbs until the stud had yielded, then increments of approximately 5,000 lbs were used until failure occurred (Specimens M4 and M5).

In specimens O4 and O5 the stud had yielded at the end of the first cycle (5,000 lbs). Therefore, in the remaining specimens a smaller load increment was used to more accurately determine the force that caused the stud to yield.

As a result of these tests, the following information for both Type 1 and Type 2 specimens was obtained. This information is qualitatively illustrated in Fig. 4.21.

- In the three specimens (O6, M4 and M5) where the load causing stud deformation was discernable, this load ranged from 1,500 to 2,000 lbs. The amount of deformation at this load was less than 0.0625 in, although there was additional displacement associated with the stud and sleeves coming into bearing.

- Slight damage to the bottom sleeve was first detected between 10,000 and 15,000 lbs.
- Damage to the top sleeve was observed in two forms: warping of the top washer and visible ovalization of the inner washer. Damage to the top sleeve was first observed over the broad range of 10,000 to 36,000 lbs.
- Damage to the bottom face sheet was first detected in the range of 20,000 to 36,000 lbs.
- Only the two specimens with the Type 2 connection displayed damage to the top face sheet and in both specimens this occurred after loading the specimen to 25,000 lbs.
- The maximum load resisted by the specimens with the Type 1 connection ranged from 32,000 to 36,000 lbs while the maximum load attained in the specimens with the Type 2 connection was 25,000 lbs in both specimens. However, in one of the specimens using the Type 2 connection, failure did not result from the inability for the specimen to sustain any additional force, but rather, excessive deformation of the stud prevented reassembling the specimen after inspection.

Also during this phase of testing, the deformation of the stud was measured after each increment of loading. This was done using a level and carefully measuring the difference in height between the one side of the base of the stud and the same side of the tip of the stud. While this data is subject to error, one noticeable trend that was observed was a slope change, similar to the LVDT load-displacement results, which occurred at

approximately 10,000 lbs. Therefore, it is assumed that the displacement in the ultimate load specimens (Fig. 4.20) is largely due to stud deformation, as the plots followed the same trend as those of Fig. 4.20.

4.5 Summary and Conclusions

The primary purposes of this phase of testing were to determine the static shear strength of the connections studied, to evaluate the amount and type of damage incurred by the components of the connection, and to study the general behavior of the connections in order to select a final design to be used in the next phase of testing. As a result of this investigation, the following conclusions were made.

- Specimens with the Type 3 connection exhibited much lower ultimate strengths than the specimens with the other two sleeve designs. Furthermore, examining the panel of the specimens that contained the Type 3 connection after testing revealed that the damage to the bottom face sheet was more severe than that of the other specimens. These facts indicate the bottom sleeve is a critical component of the connection in order to distribute the force transferred by the stud to a larger surface area and subsequently reduce the stress in the bottom face sheet.
- The displacement of the specimen is primarily due to deformation of the stud. In addition, there is also some small displacement of the panel relative to the stud, until the sleeves and stud come into bearing (when

grout is not used). Crushing/ovalization of the bottom sleeve and bottom face sheet also contributes to the specimen displacement.

- The load vs. displacement plots for the specimens using the Type 1 and Type 2 connections show that the data follows two distinct slopes and the transition between these two slopes occurs at approximately 10,000 lbs. After carefully reviewing the test data and considering the results of the damage evaluation tests, it appears that the increased stiffness that occurs at approximately 10,000 lbs is a result of the bottom sleeve coming into contact with the stud. The fact that 10,000 lbs was also the load level at which damage to the bottom sleeve was first observed in the damage evaluation tests supports the conclusion that this load is approximately the load level where the stud and bottom sleeve came into contact. The increased stiffness results because, once there is contact between the stud and bottom sleeve (in addition to the initial point of contact with the inner washer), the applied load is transferred to the stud through two points of contact, one at its base and one near its end. This loading situation would obviously cause less deformation than the initial loading situation of the stud being loaded only near its end.

  Because the Type 3 connections did not contain a bottom sleeve, there is a less pronounced change in slope at 10,000 lbs in these specimens. It is believed the stud and bottom face sheet came into contact at this level of load as in the other specimens. However, because the bottom face sheet is not as stiff as the steel bottom sleeve used in the other connections, there

is not the significant increase in stiffness that is apparent in the other types of connections.

For the grouted specimens, the load vs. displacement plot clearly shows one consistent slope that is approximately equal to the slope of the Type 1 and Type 2 connections after contact with the bottom sleeve occurred. It is felt that this is because the grout allows for uniform loading of the stud throughout the loading range, which is similar to the mode of load transfer in the other connections after contact with the bottom sleeve. It is also noteworthy to mention that there is not a significant increase in stiffness when grout was used. This indicates that the grout does not behave compositely with the stud.

- From the results of this study, it was determined that the Type 1 connection provides the best connection of those investigated when ultimate load and relative amount of damage to the connection components are considered. Therefore, this is the connection that was selected for use in the system level testing, which is the next phase of this research.

Table 4.1: Summary of Results from Ultimate Load Tests

Specimen Description	Sample	Ultimate Load (kips)
Type 1 Connection	O1	37.3
	O2	31.7
	O3	37.2
Type 2 Connection	M1	33.4
	M2	31.2
	M3	32.4
Type 1 Connection	R1	16.3
	R2	14.5
	R3	20.0
Type 1 Connection with Grout	G1	33.2
	G2	31.5

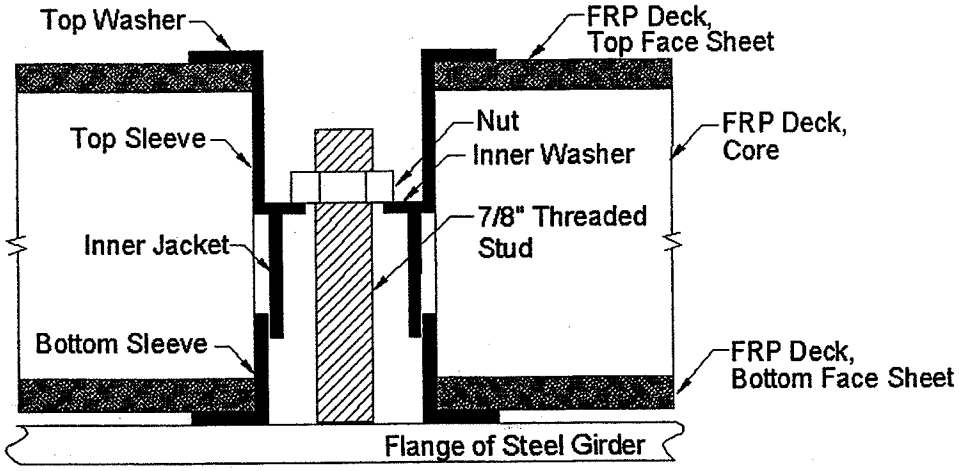

Figure 4.1: Panel Connected to Girder with Type 1 Connection

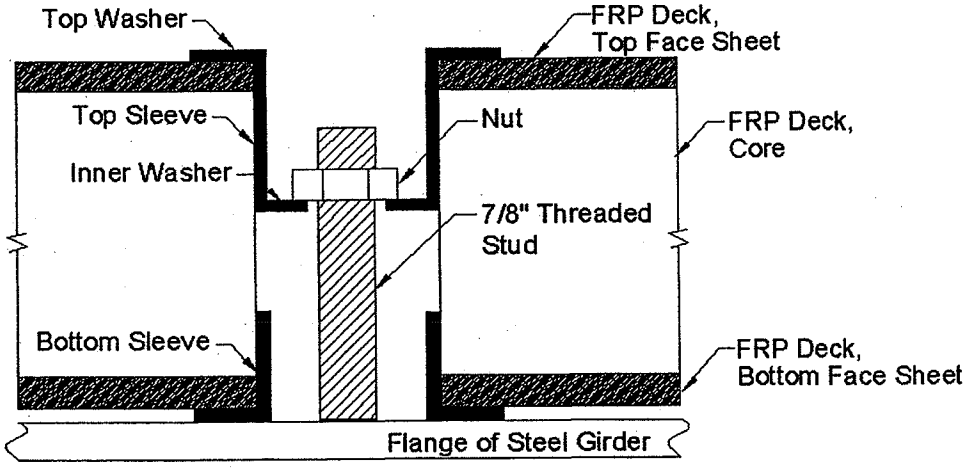

Figure 4.2: Panel Connected to Girder with Type 2 Connection

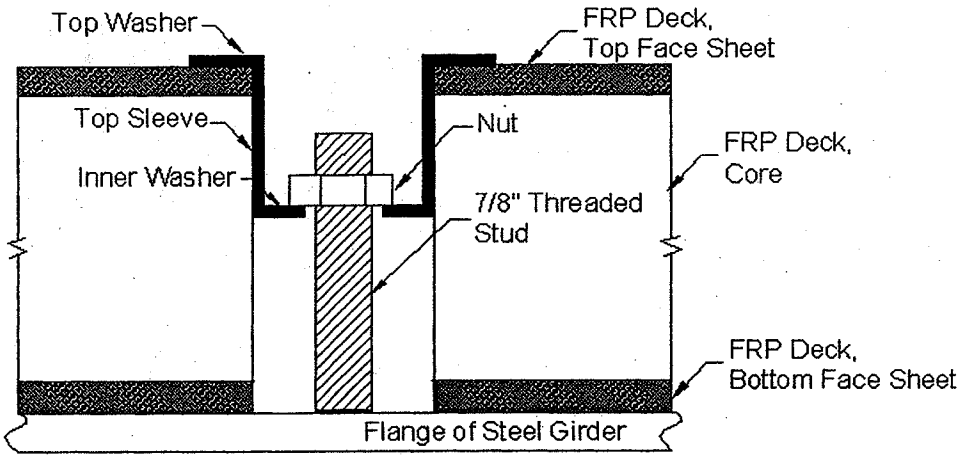

Figure 4.3: Panel Connected to Girder with Type 3 Connection

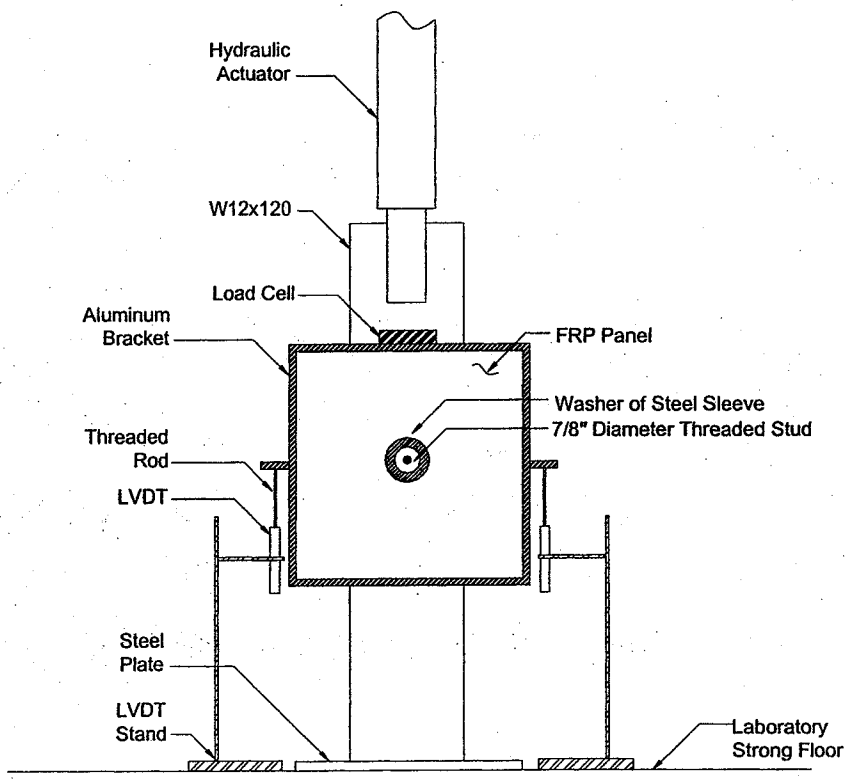

Figure 4.4: Testing Configuration for Static Connector Strength

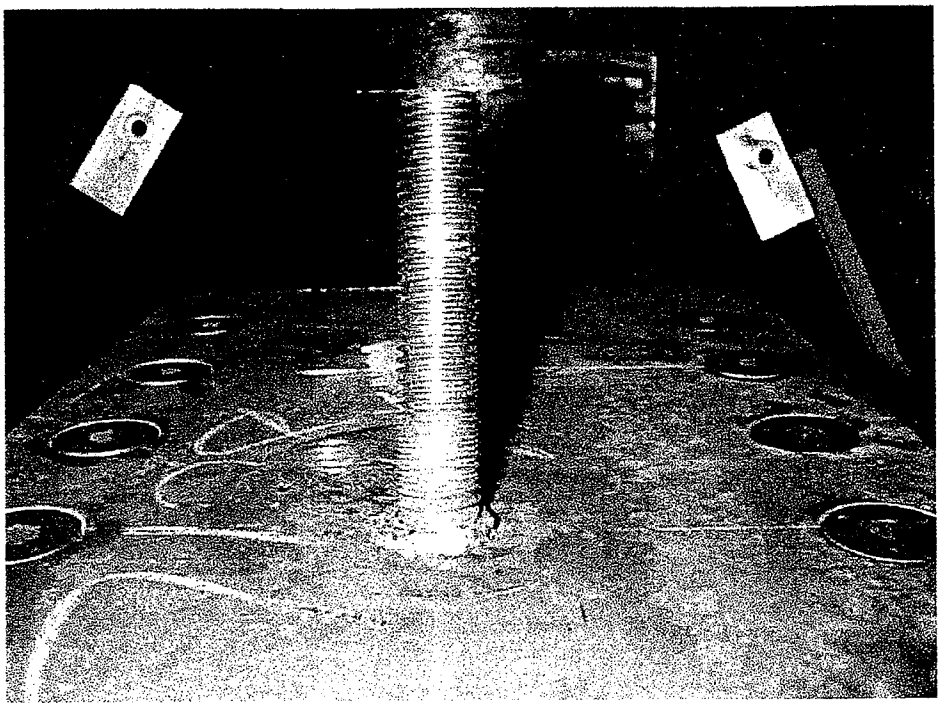

Figure 4.5: Steel Plate Bolted to Column (From Above)

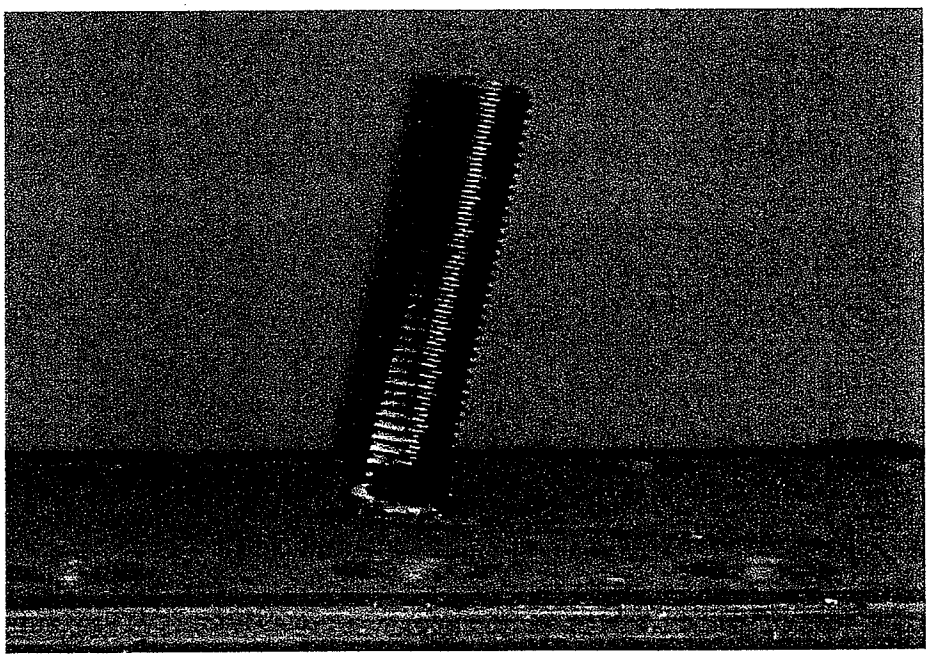

Figure 4.6: Typical Deformation of Stud After Loading

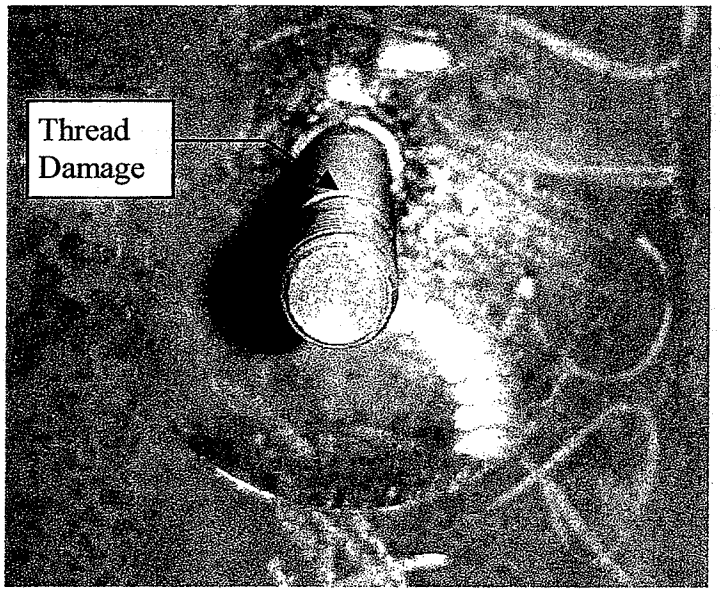

Figure 4.7: Deformation of Threads due to Contact with Inner Washer

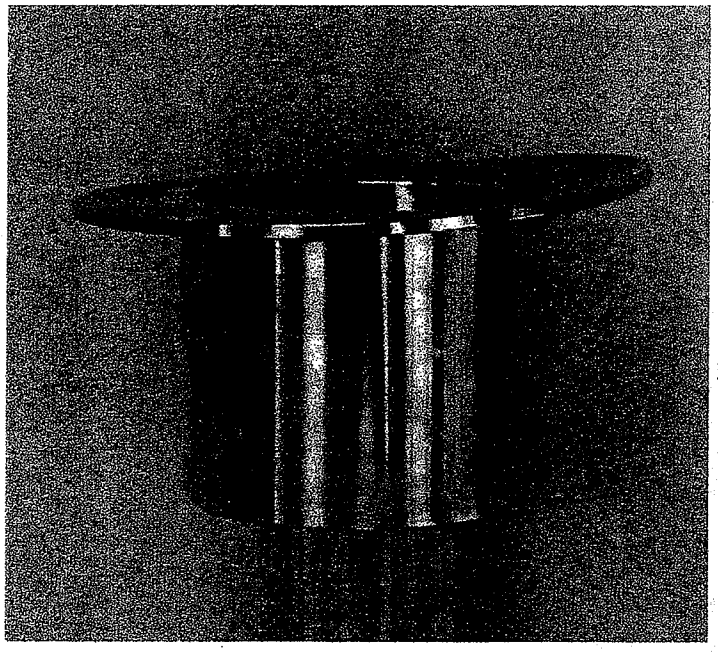

Figure 4.8: Warping of Top Washer
(Type 3 Connection)

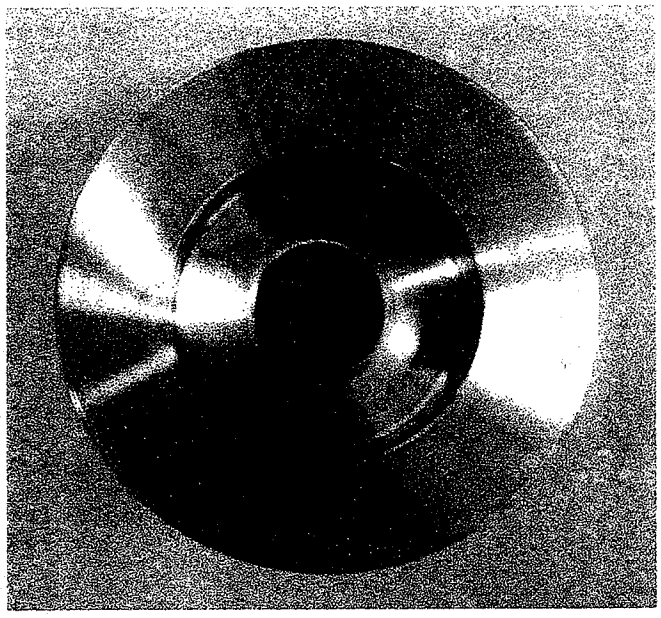

Figure 4.9: Typical Ovalization of Inner Washers

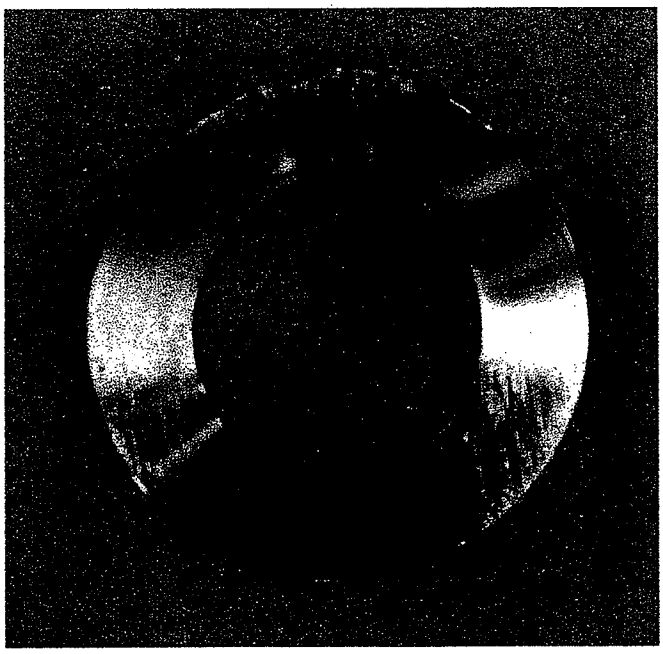

Figure 4.10: Typical Deformation of Bottom Sleeve

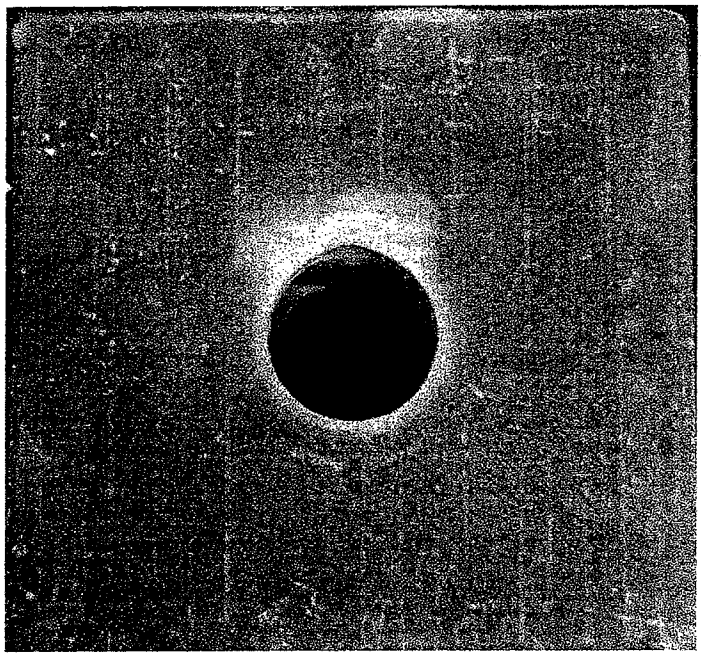

Figure 4.11: Typical View of Bottom Face Sheet after Loading

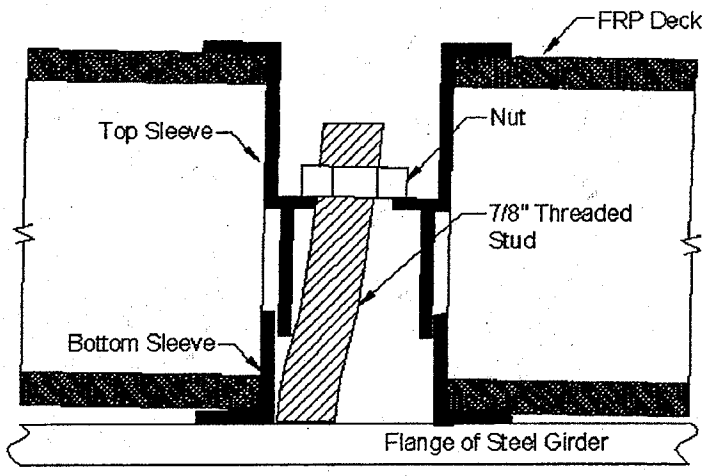

Figure 4.12: Specimen Position after Loading

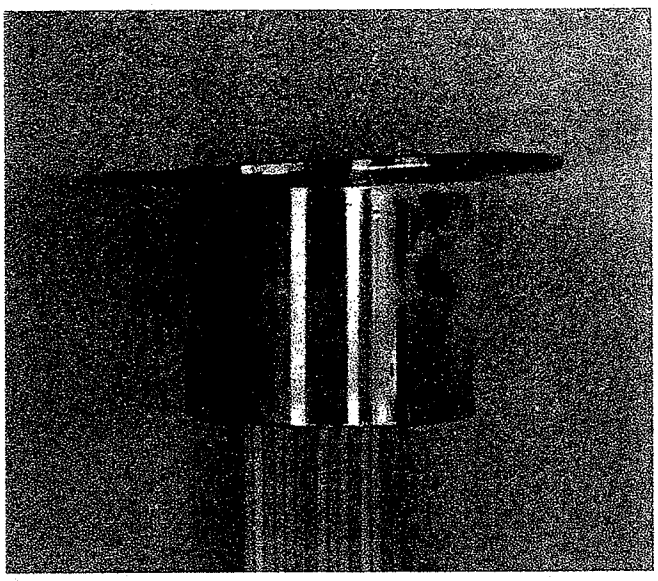

Figure 4.13: Warping of Top Sleeve
(Type 2 Connection)

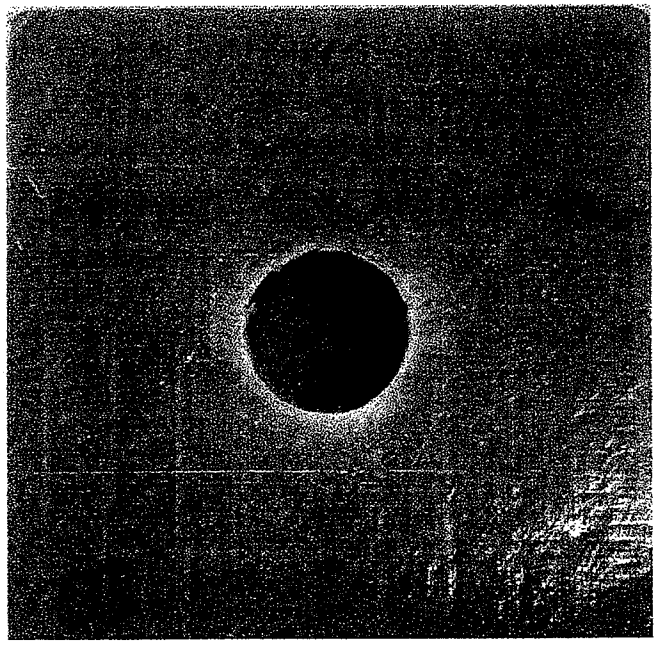

Figure 4.14: Typical Damage to Top Face Sheet in Specimens
Using Type 1 and Type 2 Connections

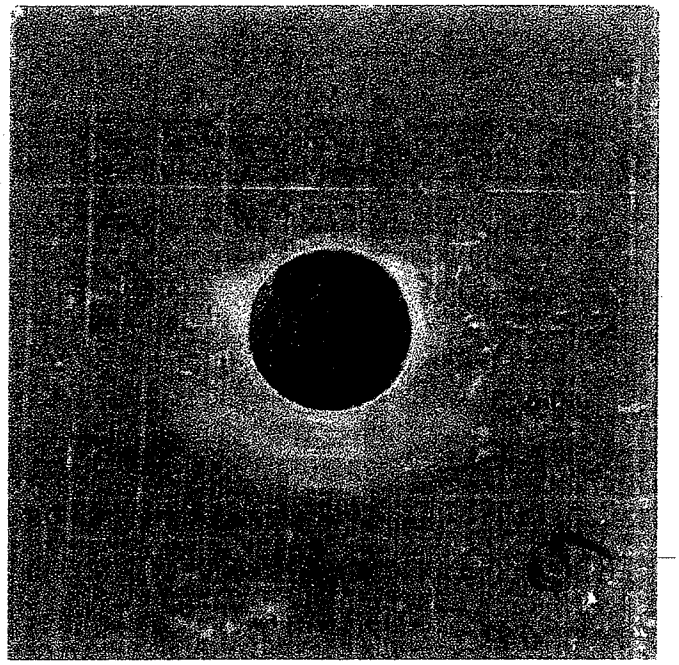

Figure 4.15: Typical Damage to Top Face Sheet in Specimens Using Type 3 Connection

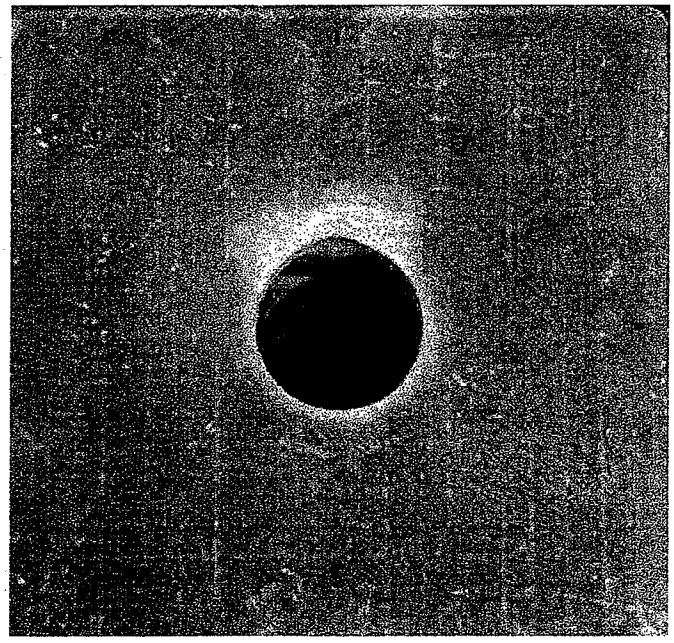

Figure 4.16: Typical Damage to Bottom Face Sheet in Specimens Using Type 1 Connection

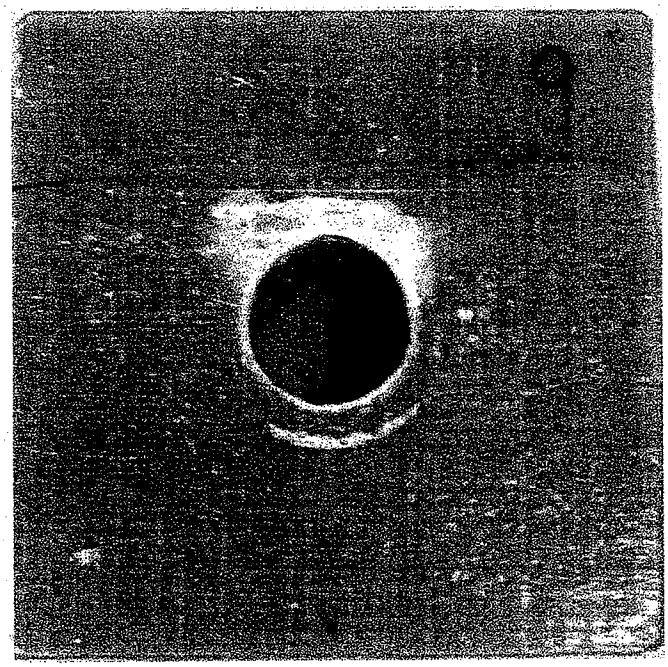

Figure 4.17: Typical Damage to Bottom Face Sheet in Specimens Using Type 2 Connection

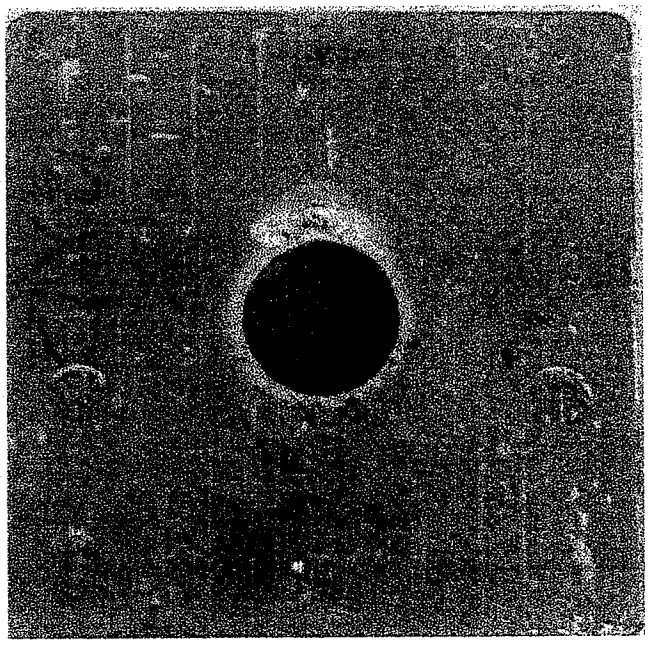

Figure 4.18: Typical Damage to Bottom Face Sheet in Specimens Using Type 3 Connection

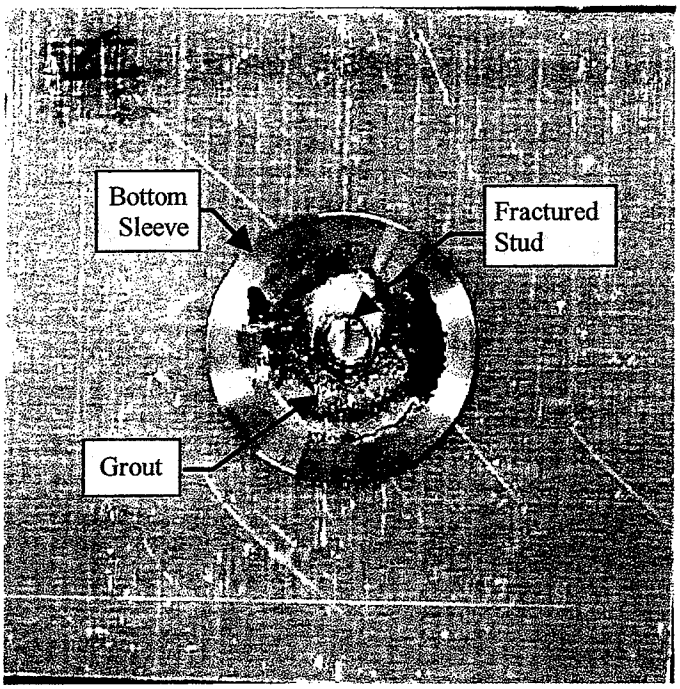

Figure 4.19: Typical View of Bottom Face Sheet
of Grouted Specimen After Testing

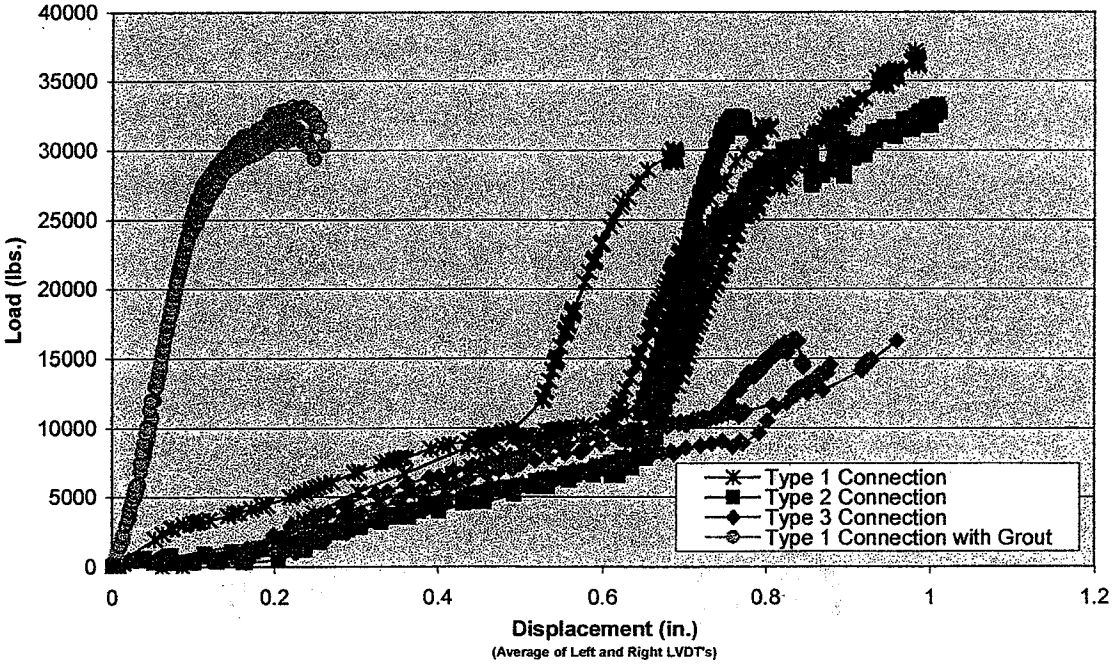

Figure 4.20: Load vs. Displacement
For Ultimate Load Specimens

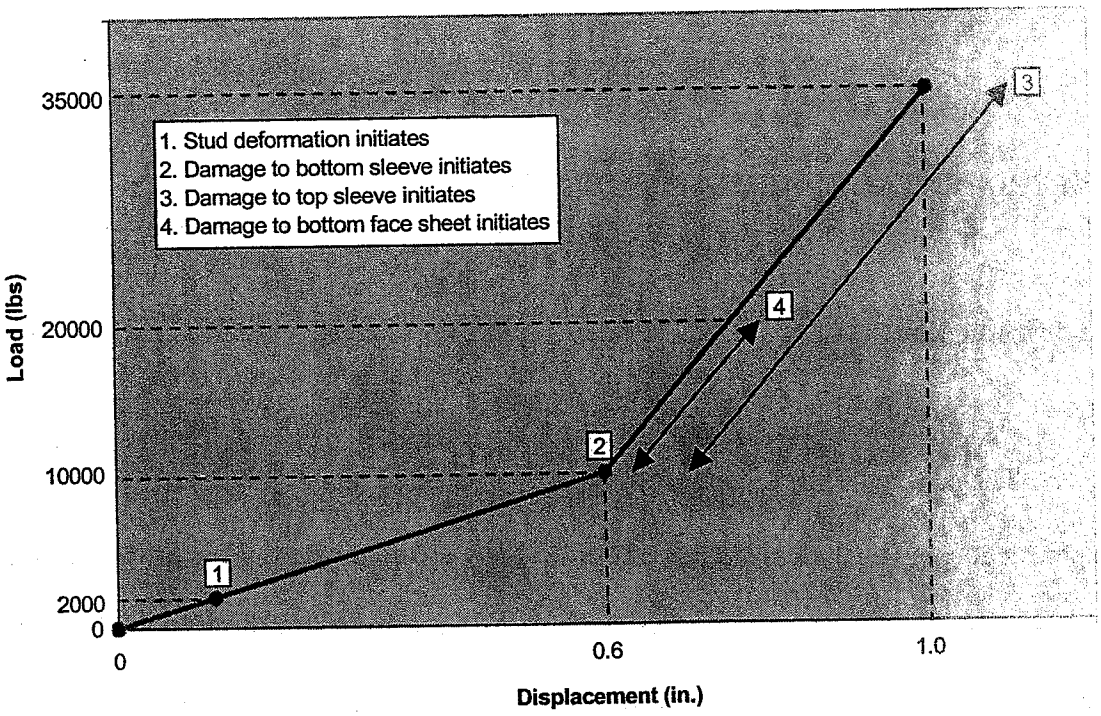

Figure 4.21: Idealized Summary of Damage to Components Observed during Damage Evaluation Tests

Chapter 5

EXPERIMENTAL EVALUATION OF SYSTEM MODEL

5.1 Introduction

The selected Type 1 connection was implemented in a reduced scale bridge and experimental and analytical studies of this bridge were conducted. This bridge consisted of three steel girders 24 ft in length and a FRP deck comprised of three panels approximately 8 ft in length. The connection that was selected in Chapter 4 (Type 1) was utilized to connect the deck to the girders at approximately 4 ft intervals. The threaded stud of the connection was welded to the supporting girders using a Miller stud welding gun. Cross bracing was provided between the girders at the supports and midspan using $3x3x^3/_8$ steel angles, and the angles were fastened to the ½ in. thick stiffeners using $^5/_8$ in. diameter A325 structural bolts. In addition, a bolt was installed in the center of each angle, joining the two angles of a cross frame together. Both finite element modeling and experimental testing of this bridge were performed. The finite element portion of this study is discussed in Chapter 6 and this chapter discusses the experimental testing.

5.2 Bridge Configuration and Instrumentation

The geometry of the scale bridge is shown in Fig. 5.1 and Fig. 5.2 shows a photograph of the test setup. In summary, a 24 ft simple span bridge was constructed using three W24x55 A572 Grade 50 steel beams, a FRP deck comprised of three 117 in. x 98 in. x 5 in. panels, and several of the selected Type 1 connections. Simply-supported boundary conditions were created by utilizing a pinned support at one end of the beams and a roller condition at the other. The pinned supports consisted of a steel plate with a 1.5 in. diameter rod welded parallel to one side of the plate and a threaded rod welded perpendicular to other side (see Fig. 5.3-a). The threaded rod is then inserted into the center of a load cell, which is used to record the reaction force at each end of the beam. The roller supports were manufactured in a similar manner, except that the steel rod was not welded in place; instead, the rod was free to move inside of a groove cut in the plate (see Fig. 5.3-b). The load cells were placed on large concrete supports at 54 in. spacing and then the girders were set into position. By recording the reaction force at each support, information can be obtained regarding load distribution characteristics.

Load was applied using a MTS 110 kip servo-hydraulic actuator that was mounted to a large structural frame as shown in Figs. 5.2 and 5.4. A load of 20 kips (equal to the heaviest single wheel load for a HS25 vehicle) was applied at the center of the bridge over a 24 in. by 9.5 in. contact area using a 2 in. thick steel plate. The contact area was chosen to approximate the wheel contact area of a standard HS25 vehicle, where the 24 in. direction of the plate is placed parallel to the girders. A constant load rate of 2

kips per minute was used for all tests and all testing was conducted within the linear elastic range of the materials.

In addition to recording the reactions at the supports, deflections were also recorded at regular intervals throughout the loading phase. These measurements were recorded using linear variable differential transformers (LVDTs) at the nine locations indicated in Fig. 5.5. Due to limitations of the data acquisition system used, data could not be recorded from all of the LVDTs at one time. Therefore, it was required to perform the test three times in order to obtain the deflections at all of the desired locations. However, during all three tests, data was recorded from a common LVDT (location 4) in order to assure compatibility of the results.

5.3 Results

Results of the experimental testing are presented in Table 5.1. Note that series 1, 2, and 3 refer to the three times the test was performed in order to obtain all of the required data. Shown in the table are the reactions at each of the six supports and the deflections at the nine points indicated in Fig. 5.5. Also shown in the table is the average result for each data point and the percent error between the results obtained from each part of the test.

Even though the data presented was obtained by loading the bridge three separate times, compatibility of the results is assured by examining the percent error between the different series. As shown in Table 5.1, the maximum percent error between any two tests is 2.2% (deflection #9). However, it is noteworthy to mention that although this is

the maximum percent error, the deflection at location #9 from the two measurements is identical when reported to the thousandth of an inch. Because of the small percent error obtained when comparing the results from the three different test series, it is believed that one can neglect the fact that the data was obtained from three series, and the average results may be used with sufficient confidence.

Due to symmetry, several of the resulting reactions and deflections should be the same. For example, the reactions at each end of the interior girder (R3 and R4) should be identical. However, these two reactions differ by 0.066 kips. Also, all of the reactions at the exterior girders (R1, R2, R5, R6) should be equal; instead, there is a difference of 0.316 kips. Other results that should be equal under ideal conditions are: deflections 1, 3, 7, and 9 (difference of 0.006 in.), deflections 2 and 8 (difference of 0.026 in.) and deflections 4 and 6 (difference of 0.016 in.). These discrepancies may be attributed to several sources.

- First, although every effort was made to place the load at the center of the bridge, it is likely that the load was slightly misplaced.
- Additionally, it is possible that some of the sensors may have been misaligned. Again, while care was taken to place all of the load cells and LVDTs at their specified locations as accurately as possible, the actual position of the instrumentation may have deviated slightly from the intended location.
- The accuracy of the instrumentation used may also contribute to the experimental error. The LVDTs are believed to be accurate to the reported number of significant digits, however the reaction data is reported to the nearest pound, which is of higher precision than the load cells are capable of capturing.

- The anti-symmetric results may also result from the relative tightness of the connections used to secure the deck to the girders. It is thought that if some of the connections were tightened more than others, this may have influenced the manner in which load was distributed throughout the deck.
- Lastly, additional causes that may have contributed to the anti-symmetric results are the imperfections of the FRP deck. Figure 5.6 shows a significant amount of warping of one of the panels (although warping is characteristic of all three panels), which is one example of the referenced imperfections. As a result of this warping, the girders do not provide constant support of the deck panels, and instead the girders support the panels in only random locations, often over relatively short distances. While it is not possible to quantify the impact the warping of the deck may have had on the results, it is believed that the anti-symmetric qualities of the FRP panel may have contributed to the lack of symmetry obtained for the resulting deflections and reactions.

5.4 Summary

Reactions and deflections resulting from a load of 20 kips applied at the center of the reduced scale bridge have been determined. While there is some anti-symmetry of the results attributed to the sources of experimental error discussed above, there is good correlation between the data obtained from repeating the test multiple times. These experimental results will be compared to the results of the finite element analysis in the following chapter.

Table 5.1: Results from Experimental Study of Reduced-Scale Bridge

	Reactions (kips)						Deflections (in.)								
	R1	R2	R3	R4	R5	R6	1	2	3	4	5	6	7	8	9
Series 1	2.489	2.330	5.344	5.419	2.189	2.229	0.029	0.060		0.067					
Series 2	2.519	2.345	5.330	5.389	2.193	2.224				0.066	0.160	0.051	0.024	0.085	0.028
Series 3	2.496	2.316	5.364	5.429	2.173	2.222			0.023	0.067	0.158	0.051	0.025	0.087	0.028
Percent Error	**1.2**	**1.3**	**0.6**	**0.7**	**0.9**	**0.3**				**1.7**	**1.3**	**0.0**	**0.8**	**1.9**	**2.2**
Average	**2.501**	**2.330**	**5.346**	**5.412**	**2.185**	**2.225**	**0.029**	**0.060**	**0.023**	**0.067**	**0.159**	**0.051**	**0.024**	**0.086**	**0.028**

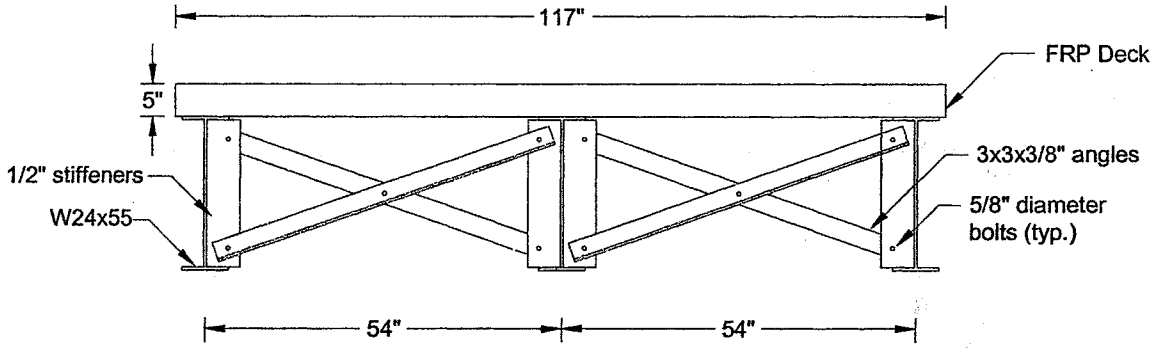

(a) Cross Section

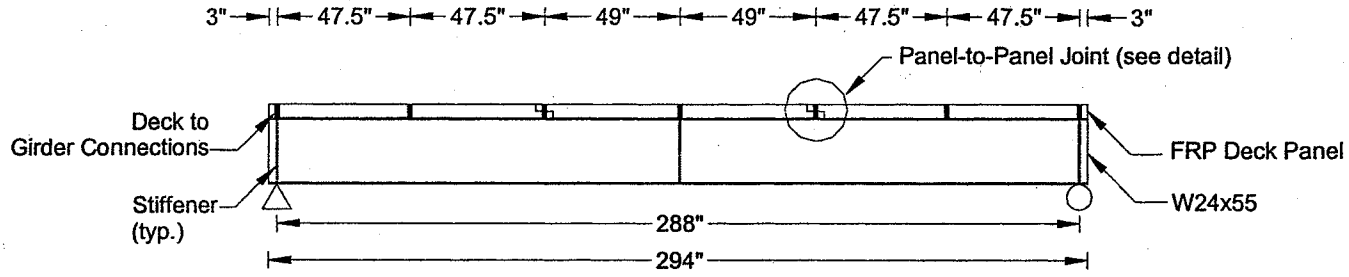

(b) Elevation View

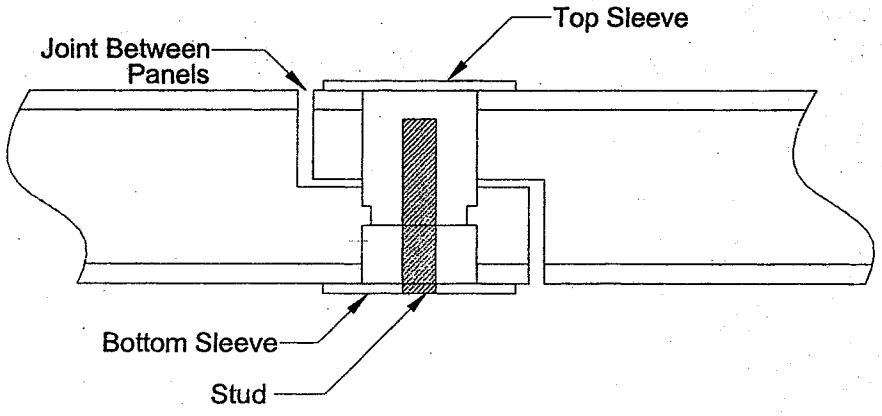

(c) Detail of Panel-to-Panel Joint

Figure 5.1: Geometry of Scale Bridge

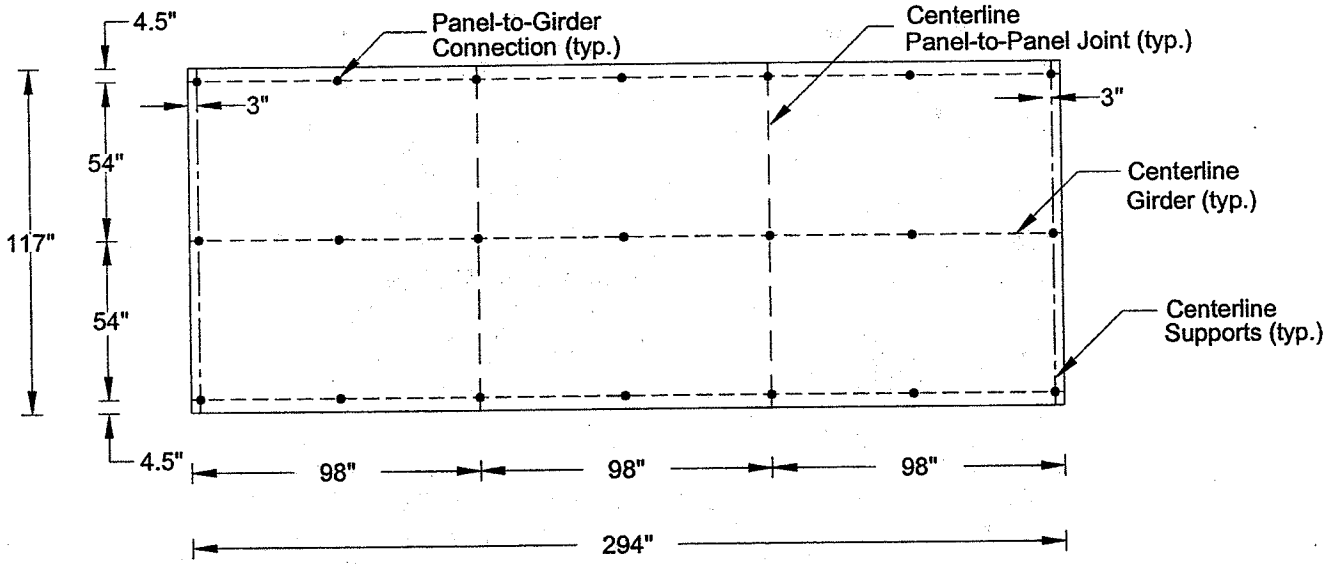

(d) Plan View

Figure 5.1: Geometry of Scale Bridge (continued)

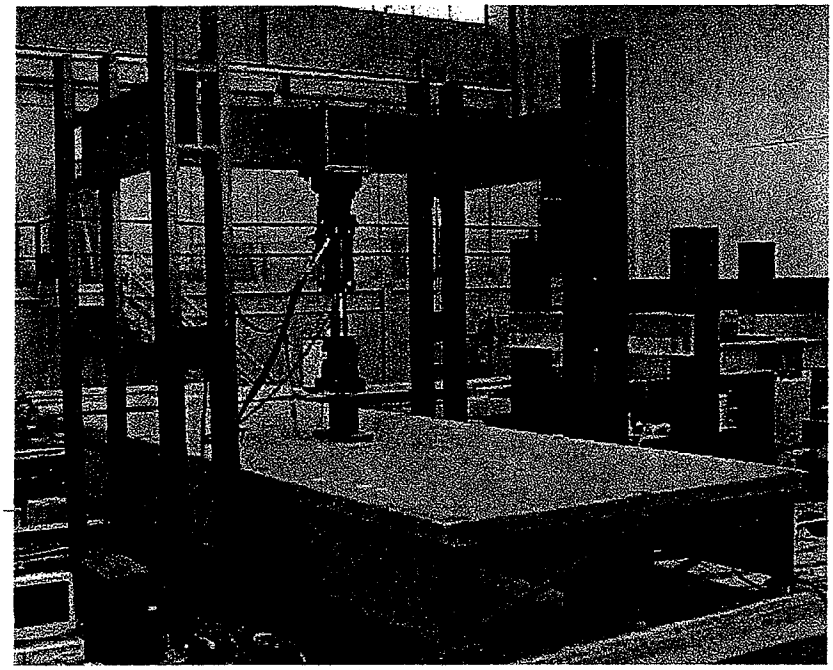

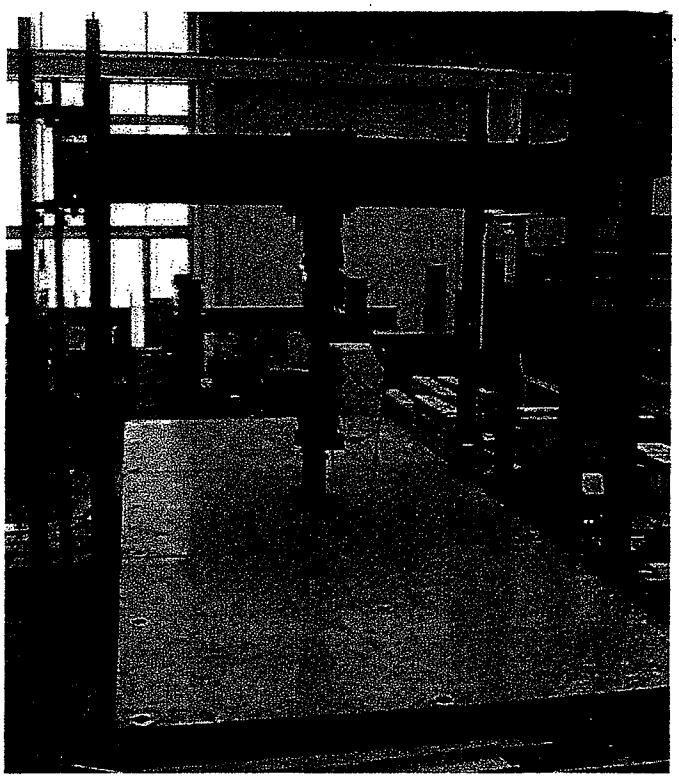

Figure 5.2: Photographs of Reduced Scale Bridge

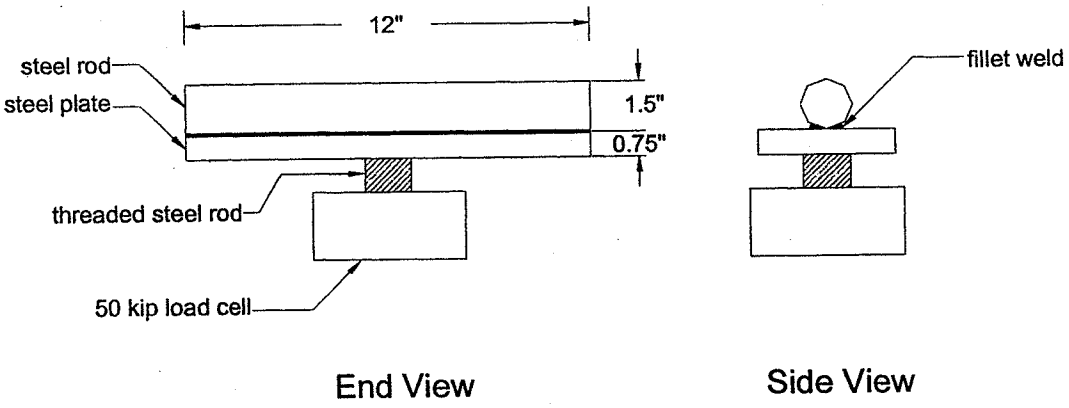

(a) Pin Support

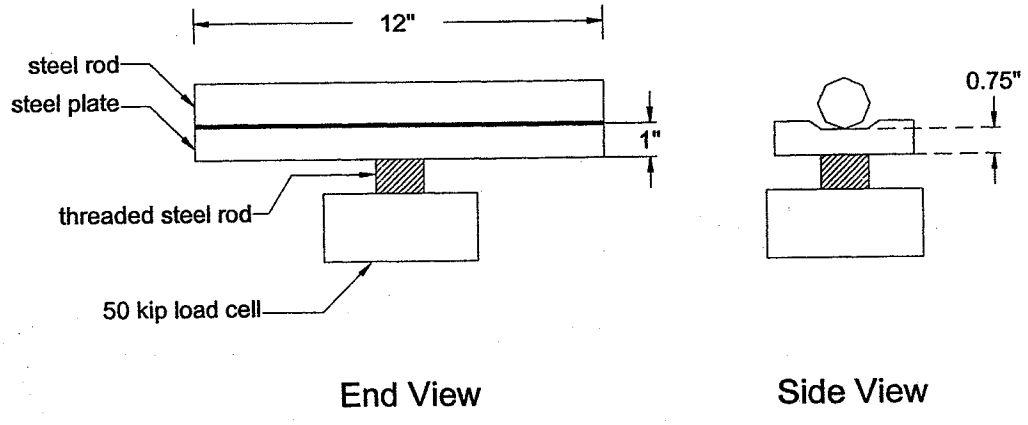

(b) Roller Support

Figure 5.3: Schematic Diagram of Pin and Roller Supports

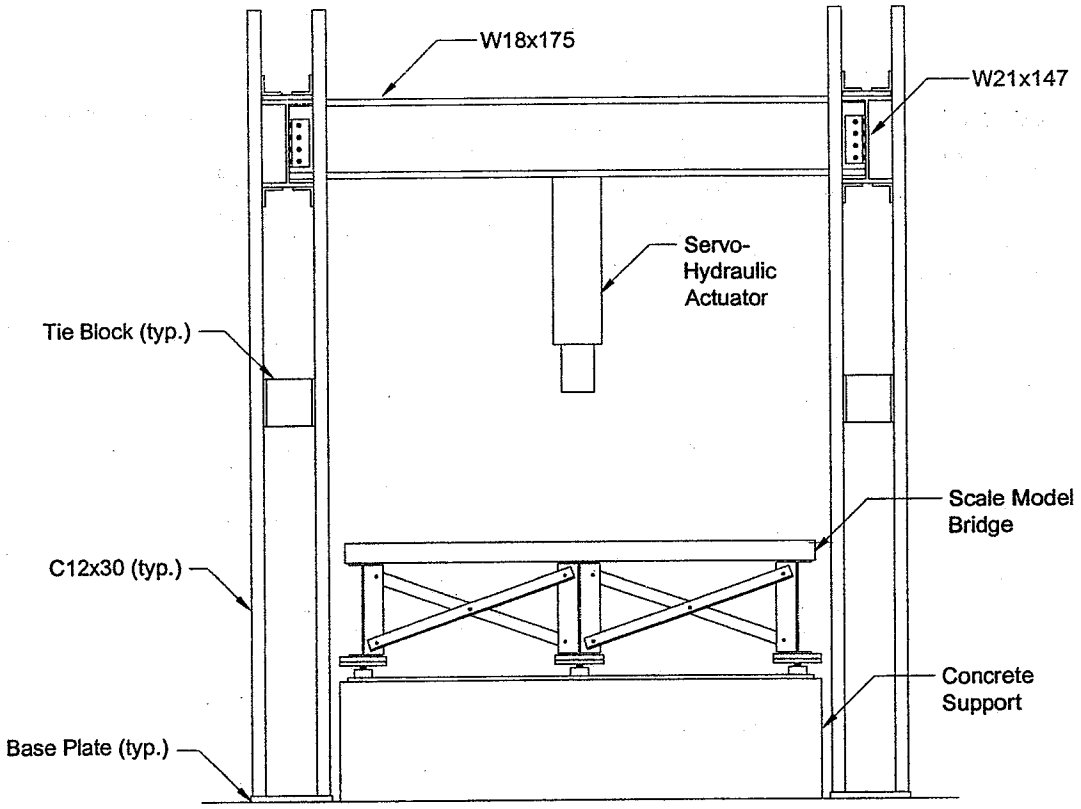

(a) Elevation View

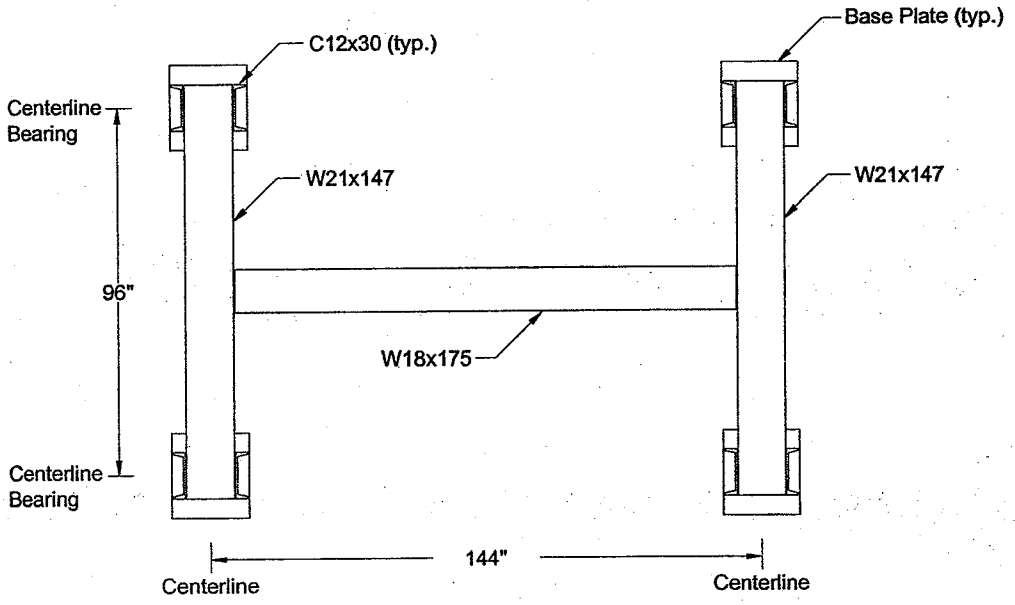

(b) Plan View
(Scale Bridge not shown in Plan View)

Figure 5.4: Structural Frame

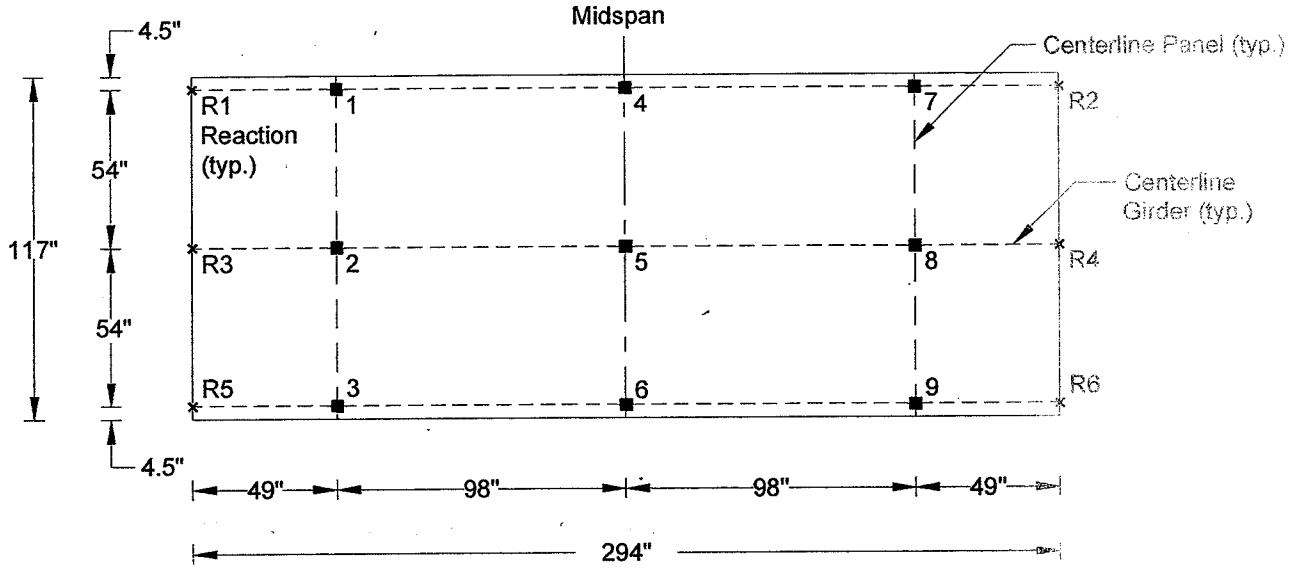

Figure 5.5: Locations and Labeling System
For Data Reported from FE and Experimental Models

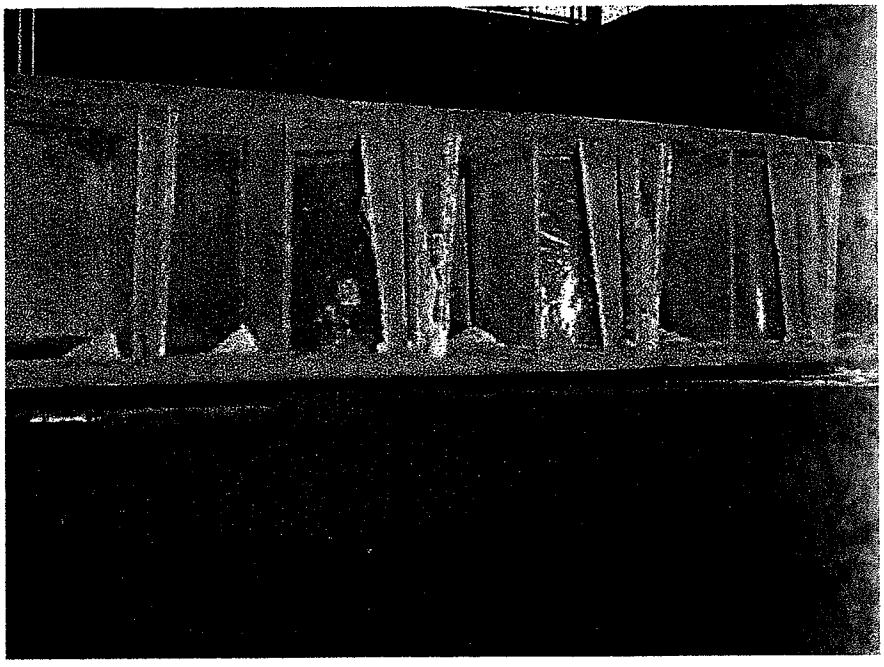

Figure 5.6: Photograph of Warping of FRP Panel

Chapter 6

FINITE ELEMENT ANALYSIS OF SYSTEM MODEL

6.1 Introduction

Upon completion of the experimental testing of the reduced scale bridge (discussed in Chapter 5), an analytical study of this bridge was also performed. The bridge consists of three steel W24x55 girders 24 ft in length, three FRP panels 8 ft in length, and twenty-one of the Type 1 connections, spaced at approximately 4 ft intervals. Additional information regarding the geometry and testing methods of this bridge are described in detail in Chapter 5, also see Fig. 5.1. The goal of the analytical study was to develop a finite element model of the bridge that accurately predicts reactions and deflections compared to the experimental results. The modeling techniques used in this study can then be used to predict load distribution characteristics and deflections for other superstructure configurations. A description of the finite element model developed, results of the study, and comparisons between the analytical and experimental results are presented in this chapter.

6.2 Finite Element Characterization of the Deck

6.2.1 Introduction

Prior to creating the model of the scale bridge, it was necessary to select a method of modeling the FRP deck. As stated previously, the FRP deck used in this research is a honeycomb-type FRP sandwich panel produced by KSCI. These panels consist of top and bottom face sheets with a honeycomb core consisting of sinusoidal and flat corrugations as shown in Fig. 1.3. Previous research efforts by Davalos et al. (2001) and Robinson (2001) have developed and verified three different modeling options (referred to as actual geometry model, 3-layer laminate model, and equivalent plate model) for this particular type of FRP deck using the finite element method.

In order to compare the accuracy of these three different methods, finite element models were created employing each of the three techniques. These models replicated a physical model of the deck that was used in previous experimental testing conducted by Robinson (2001). In the previous study, a simply supported, 180 in. by 93 in. FRP deck panel (having a 5 in. thickness) was loaded at its center with a 10,000 lb patch load, where the load was applied over a 24 in. by 9.5 in. area. Resulting deflections and strain data were recorded at key locations on the panel and comparisons were made between the data from the physical and analytical models.

For all of the finite element modeling described in this chapter, ABAQUS version 5.8 was used for analysis. In the FEA conducted by Robinson, the commercial finite element software FEMAP version 7.10 was used for pre- and post-processing, while FEMAP version 8.0 was used for the modeling performed as part of the current research.

6.2.2 Actual Geometry Model

The first method of characterizing the deck that will be discussed is the actual geometry model. In this level of analysis, each of the subcomponents of the sandwich deck are modeled. For this analysis a representative 4 in. x 4 in. "cell" element (see Fig. 6.1) is discretized and then "copied" to fill the required deck area. In the work by Robinson (2001) and Davalos et al. (2001), the 4 in. x 4 in. cell was considered to be the smallest "representative volume element" that contains all of the features necessary to fully describe the characteristics of the deck. In this model, the sinusoidal corrugations of the core are comprised of 8-node shell elements defined by parabolic curves. A mesh density of eight elements per each 4 in. section of the sinusoidal corrugation was selected, attempting to match the actual geometry as closely as possible. The flat corrugations were comprised of four 8-node shell elements for each 4 in. cell. The top and bottom face sheets were modeled using 6-node triangular laminate type shell elements. These laminate elements are created by defining 2-D orthotropic material properties for each layer used in the face sheets. The laminate elements are then defined by assigning orientation, thickness, and order of lay-up to each of these materials. The geometry of the triangular elements representing the face sheet is defined such that the face sheets and the core share coincident nodes. Reduced integration was used for all elements. Once this cell element (see Fig. 6.1) was created it was simply replicated numerous times in order to create the desired model. Because of the large computational requirements of this model, symmetry was employed by the authors to reduce the size of their model by modeling only one-fourth of the deck.

6.2.3 3-Layer Laminate Model

A second method of modeling this type of FRP deck is referred to as the 3-layer laminate model. This technique incorporates the equivalent material properties for the constituent components (i.e., face sheets and core) of the FRP deck, which have been determined by Davalos et al. (2001). These equivalent material properties for the face sheets and the core are presented in Table 6.1-a. Note that for these panels the top and bottom face sheets are identical. Using these properties, a laminate type element can then be created by simply assigning a thickness and order of lay-up to each component. Two models of this type have been created: one by Robinson and another as part of the current study. The model developed by Robinson will be discussed first.

In Robinson's 3-layer laminate model, 8-node reduced integration laminate type shell elements were used. The laminate elements were created using two different material types, one for the face sheets (2-D orthotropic material) and a separate material (3-D orthotropic) for the core. The properties used for these materials are the equivalent material properties determined by Davalos et al. (2001), which are listed in Table 6.1-a. Also, it is assumed that the applied load will cause strains that are within the elastic range of the material. Once these two materials were defined, the laminate elements were constructed by simply assigning a thickness (0.43 in. for both face sheets and 4.14 in. for the core) and order of lay-up to these materials. The element size selected was 4 in. square elements.

A finite element model of the FRP deck panel using the 3-layer laminate model was also constructed as part of the present study. This model was created using the same material properties and element type as those used by Robinson. However, 4-node

elements were used instead of 8-node elements. A second difference between the two 3-layer laminate models was the mesh size selected. In the current study, a mesh size of 3 in. was selected for the majority of the panel and a 1.5 in. mesh was used over a 9 by 24 in. area in the center of the panel. This mesh size was selected in order to establish nodes along the centerline of the panel for convenience in obtaining data.

6.2.4 Equivalent Plate Model

The final method of modeling the FRP deck of interest is to employ the equivalent panel properties developed by Davalos et al. (2001). These material properties (presented in Table 6.1-b) effectively represent the entire deck with plate elements having one set of material properties (referred to as equivalent plate model). Again, it is assumed that the material behaves elastically for the given loading range. For this model, a 2-D orthotropic material with the equivalent panel properties listed in Table 6.1-b was created, and the elements were assigned a thickness of the total panel depth, equal to 5 in. This model also used 4-node reduced integration shell elements. The mesh density for this model was the same as in the previous 3-layer laminate model.

6.2.5 Comparison Between Models

Comparisons between these three methods of characterizing the deck and experimental results were conducted in order to determine the most appropriate method for use in the present study. Specifically, the results of interest are the deflections at the seven locations illustrated in Fig. 6.2; these locations correspond to the locations where data was recorded in the experimental testing conducted by Robinson (2001). The data

from both the physical and analytical studies is presented in Table 5.2. Also, the percent error between the experimental results and each finite element model is presented. Five sets of data are presented in this table: (1) the experimental testing results obtained by Robinson (2001), (2) data from the actual geometry model created by Robinson (2001), (3) results from the 3-layer laminate model created by Robinson (2001), (4) results obtained from the 3-layer laminate model used in the current study, and (5) data for the equivalent plate model utilized in the current effort. As can be seen from the table, all three analytical models types (actual geometry, 3-layer laminate, and equivalent plate) predict the actual behavior of the deck with reasonable accuracy for most cases, with the possible exception that deflections are overestimated in the longitudinal direction (i.e., at locations 6 and 7) when using the 3-layer laminate model. It can also be seen from the results presented in Table 6.2 that the equivalent plate model most accurately predicts the actual behavior of the deck with an average of 3% difference (and a maximum of 6%) between the experimental and analytical results, compared to an average of 5% for the actual geometry model and 9% and 7% for the two 3-layer models conducted by Robinson (2001) and in the current study, respectively. The discrepancy between the two 3-layer models is likely a result of differences in mesh density and the type of element selected (4-node vs. 8-node).

As a result of this investigation, the equivalent plate and 3-layer laminate models were both selected for use in the present study in order to make comparisons between the two techniques when incorporated into a bridge system. Because the actual geometry model was more computationally demanding and was also shown to be less accurate than

the other methods, this modeling technique was not investigated in the present scale bridge model.

6.3 Finite Element Modeling of Scale Model Bridge

During the analytical study of the reduced-scale bridge, several parameters were varied in order to determine the resulting effect on the reactions and deflections obtained from the model. For example, models were created using varying mesh densities, deck properties, and constraint conditions. As a result, a "best" method was determined and details of this model are herein discussed.

Figure 5.1 shows the geometry of the scale model bridge, which was replicated as accurately as possible in the finite element model. The girders and stiffeners were modeled using 4-node, reduced-integration shell elements (ABAQUS S4R). The girders are meshed using two elements across each flange width and four elements through the web.

The cross-frames, fabricated from 3x3x5/8-in. angles, were modeled using six beam (B3) elements to represent each member, and initially the actual angle cross-section was defined in the model. It was then found that the influence of cross-frames was more significant in the model than in the experimental testing. This was indicated by the decreased reactions at the interior girder (and increased reactions at the exterior girders) in the finite element model as compared to those obtained in the physical model, i.e., more load was being transferred away from the interior girder through the cross-frames in the finite element model. To investigate this behavior, the model was recreated without

crossframes, and as expected, resulting reactions from this model gave higher reactions at the interior girder than those obtained in the experimental results, and subsequently lower reactions at the exterior girders compared to physical testing. The results of these two models are presented in Table 6.3, which shows that these models represent an upper and lower bound for reactions when compared to those from the experimental testing. As a result, an attempt was made to more accurately model the actual stiffness of the cross-frames by reducing the cross-section of the angles; an angle size of 1.25 x 1.25 x 0.125 inches was shown to give results in closest agreement with the experimental results. Reducing the cross-section of the angles is justified because the model over-predicts the stiffness of the cross-frames as a result of fully fixed conditions at the connection between the angles and stiffeners. In actuality these conditions are not fully fixed, resulting in cross-frames that are less stiff than the model predicts. Therefore, the final model selected attempts to compensate for the increased stiffness of the cross-frames due to fully fixed connections by decreasing the cross-sectional area of the angles used to form the cross-frames.

The FRP deck was also modeled using 4-node, reduced-integration shell elements. Models of the bridge were originally created using both the equivalent plate properties and the 3-layer laminate properties. A comparison of the deflections and reactions resulting from these models showed that the models that were created using the 3-layer laminate properties of the deck yielded results that compared more favorably with the experimental results. Thus, in the selected model the deck is defined using the 3-layer laminate properties as described above in section 6.2 using laminate type elements. The element size used for the deck was 3 in. by 3 in. since this element size was shown to

give accurate results in the analysis of the deck panel tested by Robinson (2001), also discussed in the previous section.

The connection between the girders and deck was modeled using multi-point constraint (MPC) rigid beam elements at the locations where these connections existed in the physical model that constrained only the vertical degree of freedom (i.e., the girder and deck were slaved together in the vertical direction at connection locations). The MPC elements were defined by an independent node at the center of the top flange and a dependent node on the deck directly above the independent node. For the bridge model, simply supported boundary conditions were specified by constraining translation in the vertical and longitudinal directions at one support and translation in the vertical direction at the remaining supports. Load was applied to the model by placing a point load of 20 kips at the center of the deck, equivalent to the loading conditions used in the physical testing.

6.4 Results

As discussed in the previous section, the finite element model that predicts results most similar to those obtained in the experimental testing contains a reduced size of cross-frames (1.25 x. 1.25 x.0.125 inches) compared to those used in the physical testing. The resulting deflections and reactions from this model, as well as the models with the actual size cross frames and no cross frames are presented in Table 6.3. Results from the model were reported at the same locations where data was recorded in the physical model in order to make comparisons between the two studies. Specifically, the results of

interest are the reactions at the six supports (labeled as R1 through R6) and the deflections at the locations indicated in Fig. 5.4 (identified as points 1 through 9). For the points that are located on a girder, the deflection reported is that from the node along the centerline of the girder on the bottom flange.

6.5 Comparison of Finite Element and Experimental Results

Results from the selected finite element model (labeled as modified crossframes) and the experimental testing are presented in Table 6.3. Also reported in the table is the percent error between these two data sets, where the percent error is calculated as the difference between the two values divided by the minimum value. The reactions and deflections are labeled according to the labeling system illustrated in Fig. 5.5. A discussion of the discrepancies between the experimental and analytical results follows.

- It can be seen from Table 6.3 that the percent error for the reactions varies from 0 to 8%. Although, it should be noted that this size of crossframes was selected because the resulting load distribution was comparable to that from the experimental testing. Therefore, a relatively low percent error for the reactions is expected.
- The percent error for deflections at locations 1, 3, 7, and 9 (which should theoretically be equal under ideal testing conditions) varies from 2 to 15% (see Table 6.1). However, if symmetry was achieved in the experimental testing, one may assume that the resulting deflection at these four locations would be equal to the average value obtained (0.026 in.). This average value compares much more

favorably with the finite element results (0.025 in.), with a percent error of only 4% and a difference of 0.001 in.

- The deflections at points 2 and 8 should also be equal if symmetric test conditions were attained. However, deflections of 0.060 and 0.086 in. were recorded in the experimental testing, and the resulting percent error at these two locations is 6% and 51%, respectively. It is likely that if the symmetry of the experimental setup could be improved, this would reduce the percent error between the experimental and analytical results.
- A similar condition occurs at locations 4 and 6, which should also give equal deflections. Deflection values of 0.067 and 0.051 in. were obtained in the experimental testing, resulting in 29% and 1% error, respectively.
- Lastly the deflection at the centerline of the interior girder is 0.159 in. during the experimental testing, versus a predicted value of 0.126 in. from the finite element model.

In addition to the lack of symmetry in the experimental results, other sources may contribute to the discrepancy between the physical and analytical results. These sources of error have been discussed in section 5.3 when explaining possible reasons for the anti-symmetry of the results but may also be relevant to this discussion. These reasons include: load eccentricity, position of instrumentation, accuracy of instrumentation, relative tightness of connections, and deck imperfections. The deck imperfections referred to are illustrated in Figs. 5.6 (a) and (b), which show warping and manufacturing flaws in the deck panels.

6.6 Summary and Conclusions

The development of a finite element model that is used to predict resulting reactions and deflections from a reduced-scale bridge has been discussed in this chapter. The methods used to develop this model may be used to predict the load distribution characteristics and deflections from other superstructure configurations. Although, improvements may be made to the analytical model developed, this model is accurate in capturing the global system behavior of the structure and the discrepancy between the analytical and experimental results at some locations may be reduced by achieving more symmetric experimental conditions.

Table 6.1-a: Equivalent Properties for Constituent Layers of FRP Deck
(Davalos, et al. 2001)

	E_x, psi	E_y, psi	E_z, psi	G_{xy}, psi	G_{xz}, psi	G_{yz}, psi	ν_{xy}	ν_{xz}	ν_{yz}
Equivalent Properties for Face Sheets	2,850,000	1,850,000	NA	546,000	546,000	546,000	0.302	NA	NA
Equivalent Properties for Honeycomb Core	76,799	143	182,970	102	16,497	45,825	.431	2.75×10^{-5}	.169

Table 6.1-b: Equivalent Panel Properties for FRP Deck
(Davalos, et al. 2001)

	E_x, psi	E_y, psi	G_{xy}, psi	ν_{xy}
Equivalent Properties for Panel	1,273,000	803,000	236,000	.301

Table 6.2: Comparison Between Experimental and Analytical Results Using Three Different FE Models

		Displacements at 10 kips (in.)						
		1	2	3	4	5	6	7
	Experimental Results	0.97	0.98	1.00	0.97	0.97	0.83	0.82
Finite Element Results: Robinson (2001)	Actual Geometry Model	0.91	0.90	0.94	0.90	0.91	0.83	0.83
	Percent Error	7	8	6	8	7	0	1
	3-Layer Laminate Model	1.05	1.04	1.08	1.04	1.05	0.96	0.96
	Percent Error	8	6	7	7	7	13	15
Finite Element Results: Modified from Robinson (2001) and repeated in this study	3-Layer Laminate Model	1.01	1.02	1.11	1.02	1.01	0.92	0.92
	Percent Error	4	4	10	5	4	10	11
	Equivalent Plate Model	0.96	0.96	0.98	0.96	0.96	0.87	0.87
	Percent Error	1	2	2	2	1	4	6

Table 6.3: Finite Element Analysis Results

	Reactions (kips)						Deflections (in.)									Average Percent Error
	R1	R2	R3	R4	R5	R6	1	2	3	4	5	6	7	8	9	
Average Experimental Results	2.501	2.33	5.346	5.412	2.185	2.225	0.029	0.060	0.023	0.067	0.159	0.051	0.024	0.086	0.028	NA
Original Crossframes	2.709	2.666	4.590	4.662	2.702	2.672	0.030	0.048	0.029	0.063	0.105	0.062	0.030	0.048	0.030	
Percent Error	8	14	16	16	24	20	3	26	26	7	52	22	21	80	5	**23**
No Crossframes	1.939	1.939	6.122	6.122	1.939	1.939	0.020	0.065	0.020	0.042	0.146	0.042	0.020	0.065	0.020	
Percent Error	29	20	15	13	13	15	40	8	15	60	9	23	20	32	38	**23**
Modified Crossframes (1.25x1.25.1/8)	2.308	2.306	5.384	5.388	2.308	2.306	0.025	0.057	0.025	0.052	0.126	0.052	0.025	0.057	0.025	
Percent Error	8	1	1	0	6	4	15	6	6	29	26	1	2	51	13	**11**

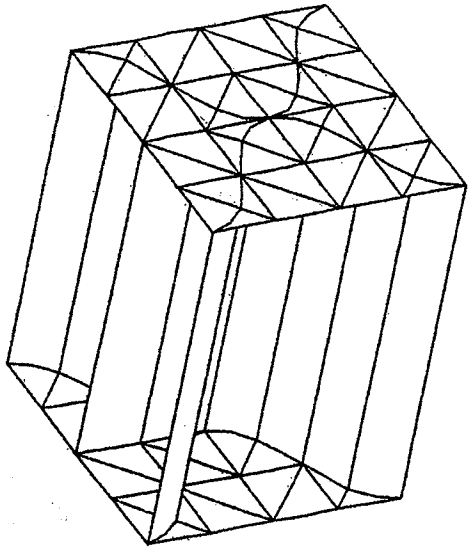

Figure 6.1: 3-Dimension View of Cell Element
Used in Actual Geometry Model of FRP Deck
(Robinson, 2001)

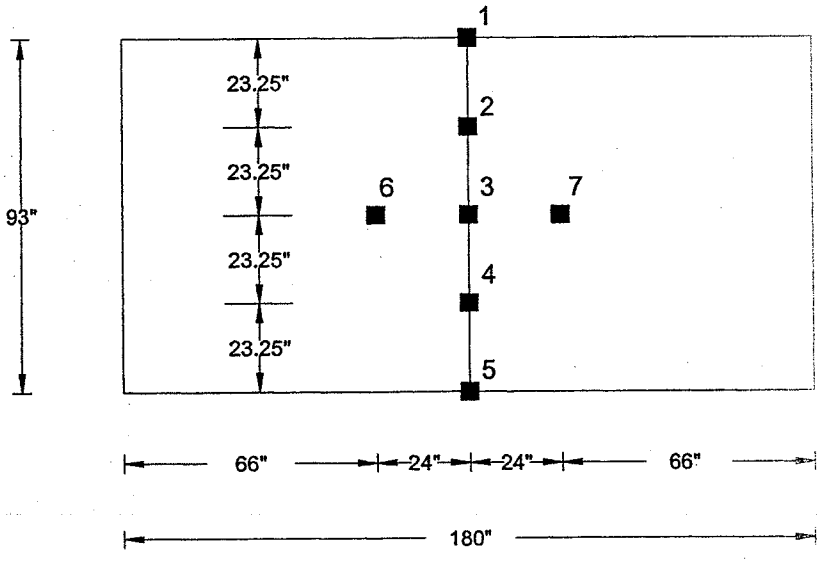

Figure 6.2: Locations Where Data is Reported for
Experimental and Analytic Studies of FRP Deck Used for
Material Modeling Purposes
(Robinson, 2001)

Chapter 7

CONCLUSIONS AND RECOMMENDATIONS

7.1 Overview of Study

This study discusses the development of a new connection for FRP bridge decks to steel girders, focusing on experimental and analytical evaluations of this connection. Specifically, the new connection was first subjected to a series of tests involving individual connectors. As a result of these tests, the average ultimate shear strength, general connection performance, mode of failure, and type of damage to the connection components was determined. Four modifications of the proposed connection were studied in this phase of testing and the design with the "optimum" performance (Type 1 connection) was selected as the final connection design.

The next phase of experimental testing implemented the selected Type 1connection in a reduced-scale bridge. This bridge consisted of three steel girders 24 ft in length, three FRP deck panels approximately 10 by 8 ft, and twenty-one of the Type 1 connections spaced at approximately 4 ft intervals. Resulting deflections and reactions due to an applied load of 20 kips (equivalent to the heaviest single wheel load for a HS25 vehicle) were determined. The reactions and deflections from the experimental study were then used to calibrate a finite element model of the reduced scale bridge.

7.2 Conclusions

As a result of the experimental testing, the satisfactory performance of the proposed connection for FRP bridge decks to steel girders was verified. The shear strength of the connection is expected to significantly exceed the shear force that the connection is expected to resist at service level loads, and the experimental tests of the reduced scale bridge verify that the connections perform well at anticipated service level loads.

The finite element model created accurately predicts resulting reactions due to an applied load at the center of the bridge within an acceptable margin of error. Also, the model accurately predicts most of the deflections, and global system behavior of the bridge is captured well. However there is a need to develop improved modeling techniques that give better correlation with all experimental results. In addition, better correlation between the experimental and analytical results may be accomplished by attempting to achieve more symmetric results in the experimental testing.

7.3 Recommendations for Future Work

It is first recommended that an attempt be made at achieving more symmetric results in the experimental testing of the reduced scale bridge. Several alterations to the previous tests are suggested that may result in improved symmetry. First, adjustments may be made to the position of the load placement and instrumentation if deemed necessary. Also, more symmetric results may be achieved by placing an elastomeric

bearing pad between the girder and FRP deck to provide constant support of the deck, compared to the intermittent support currently provided due to the warped characteristics of the deck.

Beyond the present study, fatigue testing of the reduced scale bridge is recommended in order to assess the performance of the connection under cyclic loading.

To date, this connection has been tested experimentally with only one type of FRP deck. Because the results of this study show that the shear force that can be resisted by this connection was primarily controlled by the strength of the FRP panel, this connection should also be tested with decks from other manufacturers. This should be performed using the methods discussed in Chapter 4 for individual static tests prior to using the connection with decks from other sources.

Lastly, due to the acceptable performance of this connection shown through this study, it is recommended that this connection be implemented in the field in future projects involving FRP bridge decks and steel girders.

REFERENCES

American Association of State Highway and Transportation Officials (AASHTO). Standard Specifications for Highway Bridges. Washington, 1996.

American Association of State Highway and Transportation Officials (AASHTO). LRFD Bridge Design Specifications for Highway Bridges. Washington, 1998.

American Institute of Steel Construction (AISC). Manual of Steel Construction (Load and Resistance Factor Design). Volume 2, p. 8-13. 1998.

Bakis, C.E., L.C. Bank, V.L. Brown, E. Cosenza, J.F. Davalos, J.J. Lesko, A. Machida, S.H. Rizkalla, and T.C. Triantafillou, "Fiber-Reinforced Polymer Composites for Construction – State-of-the-Art Review," *Journal of Composites for Construction*, ASCE **6**(2) (2002) 73-87. (ASCE 150th Anniversary Paper.)

Buttry, Kenneth E. Study of Composite Bridge Stringer: Behavior of Stud Shear Connectors in Lightweight and Normal-Weight Concrete. Columbia, Mo.: University of Missouri, 1966.

Davalos, J. F., P. Z. Qiao, X. F. Xu, J. Robinson, and K. E. Barth. "Modeling and Characterization of Fiber-reinforced Plastic Honeycomb Sandwich Panels for Highway Bridge Applications," *J. Composite Structures* **52** (2001) 441-452.

Easterling, Samuel W., David R. Gibbings, and Thomas M. Murray, "Strength of Shear Studs in Steel Deck on composite Beams and Joists", *Engineering Journal/American Institute of Steel Construction* **30**(2) (1993) 44-55.

Gattesco, N. and E. Giuriani, "Experimental Study on Stud Shear Connectors Subjected to Cyclic Loading", Journal of Constructional Steel Research **38**(1) (1996) 1-21.

Grant, John A., John W. Fisher, and Roger G. Slutter, "Composite Beams with Formed Steel Deck", *Engineering Journal/American Institute of Steel Construction* **14**(1) (1997) 24-43.

Hawkins, N. M., "The Strength of Stud Shear connectors", *The Institution of Engineers, Australia, Civil Engineering Transactions*, (1973) 46-52.

Hawkins, N. M. and D. Mitchell, "Seismic Response of Composite Shear Connectors", *Journal of Structural Engineering, ASCE* **110**(9) (1984), 2120-2136.

Jayas, B. S. and M. U. Hosain, "Behavior of Headed Studs in Composite Beams: Push-Out Tests", *Canadian Journal of Civil Engineering* **15**(2) (1988) 240-253.

Jayas, B. S. and M. U. Hosain, "Behavior of Headed Studs in Composite Beams: Full-Size Tests", *Canadian Journal of Civil Engineering* **16**(5) (1989) 712-724.

King, D. C., R. G. Slutter, and G. C. Driscoll, Jr., "Fatigue Strength of ½ Inch Diameter Stud Shear Connectors", *Highway Research Record* **103**(1965) 78-106.

Lloyd, R. M. and H. D. Wright, "Shear Connection Between Composite Slabs and Steel Beams", *Journal of Constructional Steel Research* **15**(4) (1990) 255-285.

Mainstone, R. J. and J. B. Menzies, "Shear Connectors in Steel0Concrete Composite Beams for Bridges. Part 1: Static and Fatigue Tests on Push-Out Specimens", *Concrete* **1**(9) (1967) 291-302.

Mainstone, R. J. and J. B. Menzies, "Shear Connectors in Steel0Concrete Composite Beams for Bridges. Part 2: Static and Fatigue Tests on Beams", *Concrete* **1**(10) (1967) 351-358.

Menzies, J. B., "C. P. 117 and Shear Connectors inSteel0Concrete Composite Beams Made with Normal-Density or Lightweight Concrete", *The Structural Engineer* **49**(3) (1971) 137-154.

Mottram, J. T. and R. P. Johnson, "Push Tests on Studs Welded Through Profiled Steel Sheeting", *The Structural Engineer* **69**(10) (1990) 187-193.

Newmark, N. M., C. P. Siess, and I. M. Viest, "Tests and Analysis of Composite Beams with Incomplete Interaction", *Proceedings of the Society for Experimental Stress Analysis* **9**(1) (1951). 75-92.

Oehlers, Deric John, "Deterioration in Strength of Stud Connectors in Composite Bridge Beams", *Journal of Structural Engineering*, ASCE **116**(12) (1990) 3417-3431.

Oehlers, Deric John, "Design and Assessment of Shear Connectors in Composite Bridge Beams", *Journal of Structural Engineering* **121**(2) (1995) 214-224.

Oehlers, D. J. and L. Foley, "The Fatigue Strength of Stud Shear Connections in Composite Beams", *Proceedings on the Institution of Civil Engineers, Part 2* **79** (June, 1985) 349-364.

Oehlers, D. J. and R. P. Johnson, "The Strength of Stud Shear Connections in Composite Beams", *The Structural Engineer* **65B**(2) (1987) 44-48.

Ollgaard, Jorgen G., Roger G. Slutter, and John W. Fisher, "Shear Strength of Stud Connectors in Lightweight and Normal-Weight Concrete", *AISC Engineering Journal* (April, 1971) 55-64.

Ramakrishna S., H. Hamada, and M. Nishiwaki. "Bolted Joints of Pultruded Sandwich Composite Laminates," *Composite Structures* **32** (1995) 227-235.

Robinson, Justin. "Analytical And Experimental Study Of FRP Honeycomb Sandwich Panels With Sinusoidal Core", Master's Thesis, West Virginia University (2001).

Slutter, R. G. and G. C. Driscoll, "Flexural Strength of Steel-Concrete Composite Beams", *Journal of the Structural Division, ASCE* 91(ST2) (1965).

Slutter, Roger G. and John W. Fisher, "Fatigue Strength of Shear Connectors", *Highway Research Record* **147** (1966) 65-88.

Toprac, A. A., "Fatigue Strength of ¾" Stud Shear Connectors", *Highway Research Record* **103** (1965) 53-77.

Viest, I. M., Siess, C. P., Appleton, J. H. and Newmark, N. M. "Studies of Slab and Beam Highway Bridges: Part IV. Full Scale Tests of Channel Shear Connectors and Composite T-Beams.", *University of Illinois Engineering Excerpt, Station Bulletin* **405** (1952).

Waddoups, M. E., J. R. Eisemann, B. E. Kaminski. *J. Composite Materials* **5** (1971) 446.

Wang J., A. Banbury, and D. W. Kelly. "Evaluation of Approaches for Determining Design Allowables for Bolted Joints in Laminated Composites," *Composite Structures* **41**(2) (1998) 167-176.